이학박사학위논문

정신증 초고위험군과 초발정신병에서 뇌 백질 네트워크의 차등적 변화

Differential changes on the white matter network of the brain in ultra-high risk for psychosis and first-episode psychosis

2015 년 8 월

서울대학교 대학원

뇌인지과학과

황재연

정신증 초고위험군과 초발정신병에서
뇌 백질 네트워크의 차등적 변화

Differential changes on the white matter network of the brain of ultra-high risk for psychosis and first-episode psychosis

지도교수 권 준 수

이 논문을 이학박사 학위논문으로 제출함

2015년 5월

서울대학교 대학원

뇌인지과학과

황 재 연

황재연의 이학박사 학위논문을 인준함

2015년 6월

위 원 장 (인)

부위원장

위 원

위 원

위 원

Differential changes on the white matter network of the brain in ultra-high risk for psychosis and first-episode psychosis

by

Jae Yeon Hwang, M.D.

A Thesis Submitted to the Department of Brain and Cognitive Sciences in Partial Fulfillment of the Requirements for the Degree of DOCTOR OF PHILOSOPHY

Director: Prof. Jun Soo Kwon

In Seoul National University, Seoul, Korea

June 2015

Approved by thesis committee:

Professor Chunkee Chung **Chairman**

Professor Jun Soo Kwon **Vice Chairman**

Professor Sang-Hun Lee

Professor Inah Lee

Professor Kim, Sung Wan

Abstract

A comprehensive figure of dysconnectivity in schizophrenia could be explored at the network level that not only accounts for local but also global organizational characteristics. However, no study has concurrently explored alteration in the white matter (WM) network of the brain of first-episode psychosis (FEP) and its prodromal stage to see whether differential changes in the structural network would exist according to the different stages of psychosis.

Thirty-seven subjects with ultra-high risk for psychosis (UHR), 21 patients with FEP, and 37 healthy controls (HC) were recruited in the study. 3-Tesla T1 structural and diffusion tensor images were reconstructed as weighted WM networks of the brain by measuring number of axonal streamlines between 82 cortical and subcortical regions. Then, graph measures extracted from the networks were compared.

Although global graph measures reflecting efficiency or small-world property of a network were not different between groups, the UHR group showed a higher assortativity coefficient compared to the FEP group and a higher modularity Q, without alteration in global clustering coefficient, compared to the HC group. At the local level, the FEP group showed a weaker WM connection between the left hippocampus and ipsilateral parahippocampal gyrus and a stronger WM connection between the left thalamus and ipsilateral superior frontal gyrus compared to the

UHR and HC groups. More rightward asymmetry of the connections between both hippocampi and ipsilateral parahippocampal gyri was seen in the FEP compared to the UHR and HC groups, and rightward asymmetry of the connections correlated positively with psychotic symptoms and negatively with level of functioning in the UHR group. The participation coefficient of the right pallidum increased in the FEP compared to the UHR and HC groups, and the measure positively correlated with nonspecific psychiatric symptoms in the FEP group.

UHR has enhanced resilience and adaptability of the WM network that may reflect highly variable prognosis of the stage among psychosis-continuum and defensive mechanism of the network against further damage. On the other hand, FEP has alteration mainly in the cortico-subcortical connectivity. These differential changes may reflect underlying biological mechanisms of developmental process leading to psychosis.

Keywords**:** ultra-high risk for psychosis; first-episode psychosis; diffusion tensor imaging; white matter; graph theory; connectome

Student number: 2010-30771

Contents

List of Tables

List of Figures

List of Abbreviations

DTI	Diffusion tensor imaging
FA	Fractional anisotropy
FDR	False discovery rate
FEP	First-episode psychosis
fMRI	functional magnetic resonance imaging
GAF	Global assessment of functioning
HAMD	The Hamilton Rating Scale for Depression
HC	Healthy controls
IQ	Intelligence quotient
MRI	Magnetic resonance imaging
PANSS	The Positive and Negative Syndrome Scale
ROI	Region of interest
UHR	Ultra-high risk for psychosis
WM	White matter

I. Introduction

1. Definition of UHR and its clinical significance

Schizophrenia is a brain disease with significant deleterious effects on a person, one's family and society (van Os and Kapur, 2009). It usually starts in the early adulthood, and has a chronic course leading to devastating effects on life of a youth. Even with successful treatment of the first psychotic episode, which could lead to complete remission from that episode, many patients would experience recurrence of psychotic episodes that, in turn, make patients not being able to manage school, job, or interpersonal relationship. The chronic, recurrent, and deteriorating course of the disorder encouraged clinicians for several decades to seek for preventive measures that might be applied even before onset of psychosis to prevent vulnerable subjects from the disease (Yung et al., 1996). Although the concept of prevention of schizophrenia was elusive when it was proposed early, prospect of preventive intervention has become more substantial recently with the advent of effective pharmacological and psychosocial interventions for schizophrenia. For this purpose, prepsychotic phase of the illness should be defined ahead of onset of psychosis.

The ultra-high risk for psychosis (UHR) criteria were developed to prospectively identify young individuals who might be at an increased risk for psychosis or schizophrenia in the near future (Yung et al., 2004). Conversion rate into psychosis is between 10 to 30% within two years after initial assessments

(Fusar-Poli et al., 2013) although initial studies reported the rate as high as 50% (Miller et al., 2002; Yung et al., 2004). Thus, research on people with UHR provides a unique stage to investigate neurobiological processes leading to psychosis or schizophrenia.

In a series of previous studies, my colleagues from the Seoul Youth Clinic, which is a specialized clinic providing comprehensive assessments and treatments to subjects with UHR at the Seoul National University Hospital, and its associated laboratory reported that individuals at UHR also exhibited similar neurobiological abnormalities of schizophrenia in a lesser degree, such as reduced cortical thickness at various brain areas (Jung et al., 2011) and deficient auditory processing (Shin et al., 2009).

2. Abnormal white matter structures in schizophrenia, UHR, and FEP

Dysconnectivity hypothesis of schizophrenia poses that the underlying etiopathological mechanism of the disorder lies in the structural dysconnection within and between brain regions (Peters et al., 2010). To address this hypothesis in vivo, diffusion-weighted magnetic resonance images were analyzed to see whether there were disorder-related abnormalities in the white matter (WM) structures of the brain. Diffusion tensor imaging (DTI) studies of schizophrenia have repeatedly

reported WM abnormalities in the brains of patients although the areas implicated were different across studies. Most commonly implicated areas are corpus callosum, anterior limb of the internal capsule, superior longitudinal fasciculus and cingulum (Adriano et al., 2010). Some studies suggest that WM abnormalities are apparent in first-episode schizophrenia patients and even in individuals at the presumably prepsychotic phase of the disorder although results are far less consistent (Peters et al., 2010). More extensive deterioration in the WM may occur after the onset of the illness. However, it is unknown which types of WM changes correspond to the processes that may underlie conversion into overt psychosis.

In this sense, specific WM deficits in some of the brain areas could not provide comprehensive understanding of the structural brain connectivity in schizophrenia. To do this, the brain should also be investigated in terms of macro-scale connectivity of the axonal brain network.

3. Network science and graph theory

Recent advances in network science provide a useful method to investigate brain network in itself (Kaiser, 2011). The graph theory modeled a brain as a graph which is composed of a set of nodes (brain regions), and edges (relationships between different brain regions). The relationships are usually defined as correlation coefficients from time-series of BOLD signals or axonal connections between brain regions.

This mathematical representation of the brain helps to investigate the global characteristics of network organization such as the degree of integration and segregation. The small-world characteristic, which appears to be a ubiquitous feature of networks of the brain (Bassett and Bullmore, 2006), could also be explored through network analysis. A small-world network typically is regionally well clustered (having a high clustering coefficient) and, nevertheless, is well connected throughout the network (having short characteristic path length) due to the presence of long-range links between separated clusters (Kaiser, 2011). This method also enables researchers to investigate network characteristics at a local level, revealing hubs within a network. Using these metrics, different conditions such as disease and health could reliably be compared.

4. Graph theoretical applications in brain diseases

Graph theoretical analyses revealed altered network structures in several brain disorders. A resting-state fMRI studies revealed that, although small-worldness and characteristic path length were not different, patients with Alzheimer's disease showed a lower global clustering coefficient than healthy controls, indicating disrupted local connectivity while preserving global connectivity in a functional brain network of AD (Sanz-Arigita et al., 2010; Supekar et al., 2008). Both structural and functional networks of the brain of patients with major depressive disorder indicated increased characteristic path length compared to healthy controls,

suggesting subtle randomization of network connectivity in the disorder (Korgaonkar et al., 2014; Zhang et al., 2011). Patients with attention-deficit/hyperactivity disorder also exhibited decreased global efficiency and increased shortest path length in the WM brain network (Cao et al., 2013). An analysis of functional brain connectivity of patients with autism spectrum disorder showed reductions in modularity and clustering, both reflecting decreased local efficiency, but shorter characteristic path lengths, reflecting increased global efficiency in the disorder (Rudie et al., 2012).

Taken together, application of graph theoretical analysis on brain disorders can shed light aberrant organizational properties of the brain in terms of global and local network characteristics of the disorders that cannot be traced with other analysis methods.

5. Abnormal network properties in schizophrenia, FEP and UHR

Previous studies employing graph theoretical measures to electroencephalography (EEG) (Micheloyannis et al., 2006; Rubinov et al., 2009) and fMRI-data (Liu et al., 2008; Lynall et al., 2010) have demonstrated abnormalities in terms of both local interconnectedness and global integrity in schizophrenia. In addition, there was a wide-spread reduction in WM connectivity

in the disorder (Skudlarski et al., 2010; van den Heuvel et al., 2010; Wang et al., 2012; Zalesky et al., 2011).

A recent study that utilized DTI method found that chronic patients with schizophrenia showed disturbed axonal connectivity among structures comprising medial frontal, parietal/occipital and left temporal areas compared to healthy subjects (Fornito et al., 2011). The other study showed that although overall small world network organization of the WM brain network in schizophrenia were preserved, disturbed connectivity was found in frontal and temporal regions in terms of increased characteristic path length of nodes in these areas (van den Heuvel et al., 2010).

However, only one study explored graph characteristics of the WM brain connectivity in first-episode psychosis (FEP) patients (Zhang et al., 2015) and no study on those characteristics was performed in individuals who are in their presumable prepsychotic phase. Moreover, studies on chronic schizophrenia did not always include important subcortical areas such as thalamus, limbic structures and basal ganglia in their network reconstruction.

6. Hypothesis and expected results

This study hypothesized that more prominent changes in the WM brain connectivity, in terms of both global and local graph measures would appear in FEP and less prominent ones in UHR compared to healthy controls, which might

indicate progressive changes in the graph measures along with transition from high-risk state to overt psychosis. At the global level, I expected decreased efficiency, small-worldness and modularity, and increased characteristic path length in FEP and, to a lesser extent, in UHR. At the local level, I expected widespread abnormalities in cortico-subcortical connections and characteristics of nodes and edges in FEP and, again, in UHR to a lesser extent.

To confirm this hypothesis, networks were reconstructed from WM tracts interconnecting both cortical and subcortical structures of the brains of UHR subjects, FEP patients, and healthy controls (HC). Then, both global and local graph measures of networks were calculated and compared.

II. Methods

1. Participants

Image data from age- and sex-matched 37 individuals at UHR, 21 patients with FEP and 37 HCs were analyzed in this study. Matching was performed by randomly selecting from larger pools of UHR subjects and healthy controls according to age and sex of the FEP patients.

UHR subjects and FEP patients were recruited from a prospective, longitudinal project to manage and investigate people at high risk for schizophrenia from the Seoul Youth Clinic (Kwon et al., 2010). The UHR group was defined according to the Comprehensive Assessment of At-Risk Mental States (CAARMS) (Yung et al., 2004) or The UHR group was defined according to the Structured Interview for Prodromal States (SIPS) (Jung et al., 2010; Miller et al., 2003). According to the CAARMS, young individuals are identified as having an increased risk for developing psychosis or schizophrenia within a short-term if they have at least one of the following risk factors: 1) attenuated psychotic symptoms, 2) brief, limited, intermittent psychotic symptoms (BLIPS) (i.e., self-resolving psychotic symptoms), or 3) vulnerability (i.e., a trait-like factor such as schizotypal personality disorder or family history of a psychotic disorder in a first-degree relative plus a recent functional decline) (Yung et al., 2004). Among UHR subjects, four patients were prescribed with antipsychotics, seven with antidepressants, and six with anxiolytics

at the time of experiment. Among UHR subjects, four (10.8%) converted into psychosis by end of March 2015. The mean duration of follow-up for the UHR subjects and mean time from enrollment to transition was 1,425 ± 338 and 667 ± 268 days.

Patients with FEP were identified if they had experienced their first psychotic episode in their lifetime, which did not overlap with the BLIPS criteria, and the onset of full-blown psychotic symptoms was less than a year at the time of enrollment. They were diagnosed as having a brief psychotic disorder, schizophreniform disorder, schizoaffective disorder, or schizophrenia with the Structured Clinical Interview for DSM-IV-TR (a text revision of the Diagnostic and Statistical Manual of Mental Disorders, fourth edition) Axis I Disorders (SCID-I). Seventeen patients were prescribed with antipsychotics, two with both antipsychotics and antidepressants, and the remaining with anxiolytics at the time of experiment.

The 37 age- and sex-matched HC subjects, without a lifetime history of any psychiatric disorder or treatment, were recruited from an Internet advertisement. HC subjects were screened using the Structured Clinical Interview for SCID-I Non-Patient Edition (First et al., 1995) with an additional exclusion criterion of any first- to third degree biological relatives with a psychiatric disorder.

Participants were excluded if they had a history of substance abuse or dependence, neurological diseases, head injury or medical illnesses with documented cognitive sequelae, or intellectual disability (IQ < 70).

All procedures were performed in accordance with the current version of the

Declaration of Helsinki. The Institutional Review Board of the Seoul National University Hospital approved all work. All subjects were provided with written informed consent including parental consent for those who were less than 18 years old. All participants of the current study were recruited from April 2010 and August 2013.

2. Clinical assessments

The Positive and Negative Syndrome Scale (PANSS) (Kay et al., 1987; Yi et al., 2001) was administered to both UHR and FEP groups to quantify psychotic symptoms. The Korean version of the Wechsler Adult Intelligence Scale (K-WAIS) was administered to all subjects to estimate their intelligent quotient. Hamilton rating scale for depression (HAMD) (Hamilton, 1960) and global assessment of functioning (GAF) was administered to both UHR and FEP groups. Because one subject in the UHR lacks clinical data, the subject was excluded when analyzing clinical data.

3. Image acquisition

MRI data were acquired using a SIEMENS TRIO 3-T scanner in the Seoul National University Hospital using a 12 channel head coil. T1-weighted 3-D

magnetization-prepared rapid-acquisition gradient echo (MPRAGE) sequence was acquired and covered the entire brain. Parameters were as follows: echo time/repetition time = 1.89/1670 milliseconds, flip angle = 9°, field of view = 250 mm, voxel size = 1.0 x 1.0 x 1.0 mm. Diffusion tensor imaging was performed using a single shot spin-echo, echo-planar sequence with the following parameters: TR/TE=11400/88 ms, b-value of 1000 s/mm2, voxel size = 1.88 x 1.88 x 3.5 mm, and 64 gradient directions.

4. Data preprocessing and network reconstruction

Using FreeSurfer (http://surfer.nmr.mgh.harvard.edu), surface meshes of the boundary between gray matter and WM from T1 images of the brain were obtained (see Fig 1. for schematic representation of whole procedure of network construction). After registering surface meshes into brains of the diffusion tensor images, the results were visually checked for possible mismatch arising from automatic registration process. Then, 34 cortical and 7 subcortical (amygdala, hippocampus, caudate, putamen, pallidum, nucleus accumbens, and thalamus) volume regions of interests (ROIs) of the gray matter for each hemisphere were generated according to the Desikan atlas (Desikan et al., 2006; Fischl et al., 2002; Fischl et al., 2004) (see Appendix for the list of ROIs).

To obtain WM tractography, eddy-current correction of diffusion tensor images using FSL (http://www.fmrib.ox.ac.uk/fsl/) was implemented as a preprocessing procedure, then deterministic fiber tracking utilizing the Fiber Assignment by

Continuous Tracking (FACT) algorithm (Mori and Barker, 1999) was performed with 35 degree of angle threshold through the Diffusion Toolkit along with TrackVis (http://www.trackvis.org/dtk/) (Wang et al., 2007). This program generates the tractography from the center of all voxels in the gray matter and WM except for ventricles.

Then, with the UCLA Multimodal Connectivity Package (UMCP, http://ccn.ucla.edu/wiki/index.php), 82 x 82 weighted connectivity matrices from the volume ROIs and tractography, in which the 82 volume ROIs was set as nodes with the number of axonal streamlines between pairs of ROIs set as edge weights, were extracted. Average connection lengths between pairs of ROIs were also calculated. The connection length of an axonal streamline is based on its actual three-dimensional trajectory. A connection length between unconnected ROIs was set as zero.

5. Graph measures

The routines from the Brain Connectivity toolbox for network measures (Rubinov and Sporns, 2010, 2011) were used except for total wiring length and laterality index. Before calculating network measures, all edge weights were normalized by dividing them with the maximum value of edge weights of networks from all study subjects, giving normalized edge weights between 0 and 1 (Rubinov and Sporns, 2010). Edge weights described below denote the normalized edge

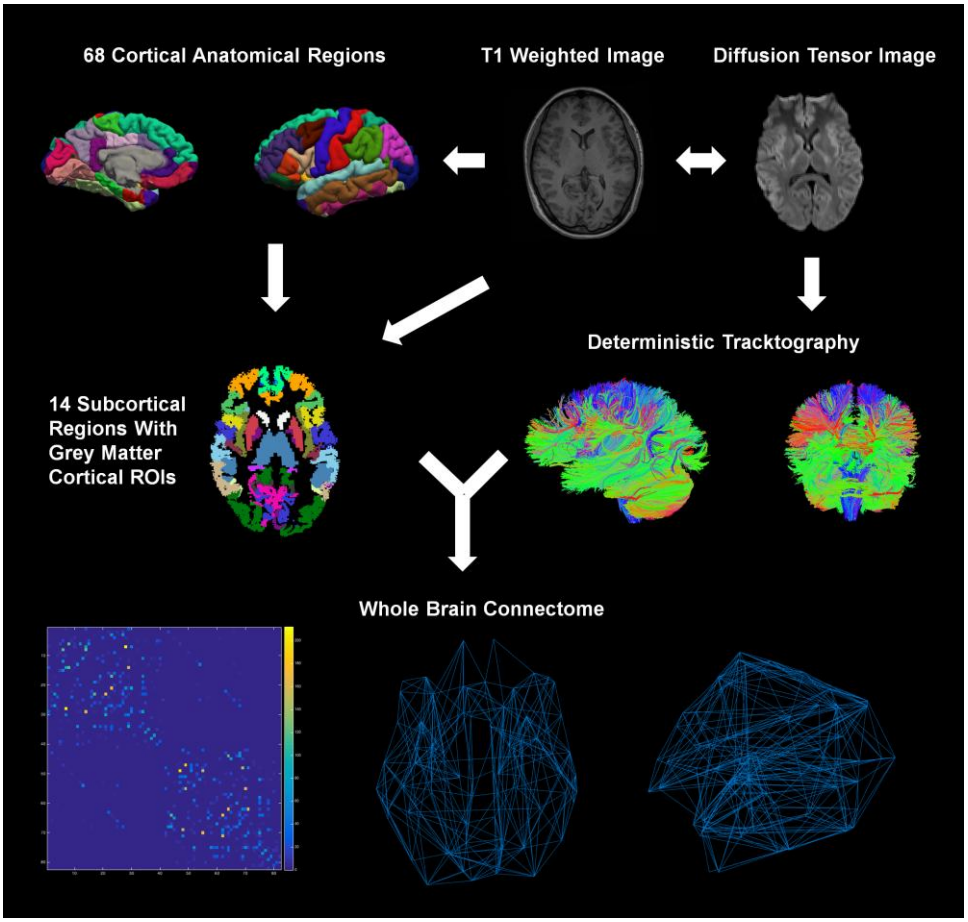

Figure 1. The procedure of network reconstruction from both T1-weighted and diffusion tensor images.

weights.

1) Edge density, nodal degree and nodal strength

Edge density represents proportion of the number of existent connections to the number of possible connections of a network. Because our network is undirected, we calculated edge density d as

$$d = \frac{E}{2(n(n-1))}$$

, where E is number of edges and n is number of nodes. The number of directly connecting nodes to a given node is its nodal degree, giving the equation

$$k_i = \sum_j a_{ij}$$

, where a_{ij} is 1 when a link (i, j) exists and 0 otherwise. The sum of weights from all connecting edges to a given node is its nodal strength (Barrat et al., 2004), giving the equation

$$k_i^w = \sum_j w_{ij}$$

, where w_{ij} is the weight of link (i, j). Another name for the nodal strength is weighted nodal degree (Rubinov and Sporns, 2010).

2) Global & local efficiency and characteristic path length

Global efficiency represents how well two nodes of a network are connected, whereas local efficiency shows how well neighbors of a node are connected (Achard and Bullmore, 2007; Latora and Marchiori, 2001).

$$E_{global} = \frac{1}{n(n-1)} \sum_{i \neq j} \frac{1}{L_{ij}}$$

$$E_{local} = \frac{1}{n} \sum_{i} E_{global}(G_i)$$

, where L_{ij}: the length of the shortest path between nodes *i* and *j* (computed with Dijkstra algorithm), N: number of nodes, Gi: the subgraph that consists of neighbors of *i* without *i* itself.

While computing the length of the shortest path between pairs of nodes, I mapped weights to distances: higher weights between a pair of nodes mean easier information transmission, thus a shorter length between them. Characteristic path length, *L*, is a global mean of shortest path L_{ij} in the brain connectivity tool box, which is slightly different from that of Watts' (1999) in that the latter uses *median* instead of *mean*.

3) Betweenness Centrality

Betweenness centrality of a node or an edge measures how many shortest paths, L_{ij}, include the node or the edge among all the shortest paths, capturing importance of the node in the network. A node or an edge with higher value may have a role of connector hubs, which connects two or more sub-networks (Brandes, 2001).

4) Clustering coefficients

Clustering coefficient is a measure of neighborhood connectivity, which shows the proportion of existing connections out of all possible connections among its neighbors. The weighted local clustering coefficient for an individual node i is

$$C_i = \frac{2}{k_i(k_i - 1)} \sum_{j,k} (w_{ij} w_{jk} w_{ki})^{1/3}$$

(Onnela et al., 2005). Global clustering coefficient is a mean of local clustering coefficients of all nodes.

$$C = \frac{1}{n} \sum_{i} C_i$$

5) Small-worldness

Small-world networks have higher clustering coefficients than random networks whereas their characteristic path length is comparable to that of a random network (Watts and Strogatz, 1998). Small-worldness S (Humphries and Gurney, 2008) was calculated as

$$S = \frac{C/C_{rand}}{L/L_{rand}}$$

, where C is the global clustering coefficient and L is the characteristic path length of the given network which were normalized by the clustering coefficient C_{rand} and the characteristic path length L_{rand} of randomly rewired networks. For each subject, 200 random graphs were generated by randomly permuting weighted edges of a

connectivitiy matrix (Bolanos et al., 2013). Then mean values of global clustering coefficient and characteristic path length for random graphs, C_{rand} and L_{rand}, were calculated for each subject.

6) Modularity, within-modular degree, and participation coefficient

Regional segregation of a network can be revealed by measures reflecting how well a set of neighboring nodes is densely connected such as clustering coefficient. On the other hand, more sophisticated measures of segregation can reveal a non-overlapping community structure within a network by subdividing the network into groups of nodes, or modules, with a maximum possible number of within-module edges, and a minimum possible number of between-module edges (Girvan and Newman, 2002). The optimal modular structure for a given network is estimated by optimization algorithm (Danon et al., 2005).

The Modularity Q is a statistic that quantifies the degree to which the network may be subdivided into clearly delineated groups. The value measures the difference between the number of edges that lie within a community in the actual network and a random network of the same degree sequence for a certain membership assignment, as follows (Newman, 2004).

$$Q = \frac{1}{l^w} \sum_{i,j \in N} \left[w_{ij} - \frac{k_i^w k_j^w}{l^w} \right] \delta_{m_i, m_j}$$

, where l^w: the sum of all weights in the network, k_i^w: a nodal strength of node *i*, and m_i: the module containing node *i*, and $\delta_{m_i,m_j} = 1$ if $m_i = m_j$ and 0 otherwise. If a particular division gives no more within-community edges than that in a random network, Q is 0. Values greater than 0.3 indicate that significant community structure exists (Newman, 2004).

Within-module degree measures degree of engagement within its participating module of a node. Weighted within-module degree z of a node is defined as

$$z_i = \frac{k_i^w(m_i) - \bar{k}^w(m_i)}{\sigma^{k^w(m_i)}}$$

, where$k_i^w(m_i)$ is a strength of a node within its participating module m_i, $\bar{k}^w(m_i)$ is average of strengths of all nodes within the module, $\sigma^{k^w(m_i)}$ is standard deviation of strengths of all nodes within the module (Guimera and Amaral, 2005; Rubinov and Sporns, 2010). To calculate a within-module degree, modular structure of a network should be identified before.

On the contrary to the within-module degree z, participation coefficient represents degree of connection beyond its participating module of a node, a different aspect of modular engagement of a node (Guimera and Amaral, 2005; Rubinov and Sporns, 2010). Weighted participation coefficient of a node y_i is defined as

$$y_i = 1 - \sum_{m \in M} \left(\frac{k_i^w(m)}{k_i^w} \right)^2$$

, where M is the set of modules, $k_i^w(m)$ is a strength of a node within each module m. The participation coefficient of a node is zero if all edges connecting the node are within its own module, and close to one if its edges are widely distributed among all modules.

7) Weighted assortativity coefficient

Assortativity coefficient, a measure of resilience, is a correlation coefficient between degrees of all nodes on two opposite ends of a link (Rubinov and Sporns, 2010). A network has high assortativity if the nodes in the network that have many connections tend to be connected to other nodes with many connections (Newman, 2002). Similarly, a network with high weighted assortativity tends to have a high-weighted link between nodes with similar degree (Leung and Chau, 2007). Weighted assortativity coefficient r^w was calculated as

$$r^w = \frac{l^{-1}\sum_\phi(w_\phi \prod_{i\in F(\phi)} k_i) - \left[\frac{H^{-1}}{2}\sum_\phi(w_\phi \sum_{i\in F(\phi)} k_i)\right]^2}{\frac{l^{-1}}{2}\sum_\phi(w_\phi \sum_{i\in F(\phi)} k_i^2) - \left[\frac{H^{-1}}{2}\sum_\phi(w_\phi \sum_{i\in F(\phi)} k_i)\right]^2}$$

, where w_ϕ is the weight of ϕth link, $F(\phi)$ is the set of the two nodes connected by the ϕth link, and H is the sum weights of all connections from a network. Networks with positive assortativity coefficient are likely to have a relatively resilient core of mutually interconnected high-degree hubs. On the other hand, networks with

negative assortativity coefficient are likely to have widely distributed thus vulnerable high-degree hubs (Rubinov and Sporns, 2010).

8) Laterality index

For any of paired measures across the midline of the brain, laterality index was calculated to see changes in asymmetrical specialization of the brain according to groups with the following equation.

$$Laterality\ Index = \frac{measure_L - measure_R}{measure_L + measure_R}$$

, where $measure_L$: the left-side value of paired measures; $measure_R$: the right-side value of paired measures. Zero means complete symmetry of that paired measures whereas -1 and +1 mean complete leftward and rightward laterality respectively.

9) Total wiring length

Total wiring length of a network is calculated as

$$W = \frac{1}{2}\sum_{ij} w_{ij} l_{ij}$$

, where w_{ij} is weight of a given edge and l_{ij} is an average connection length between ROIs based on an actual three-dimensional trajectory of a streamline corresponding to a given edge.

6. Statistical analysis

1) Comparison of demographic variables and global network properties

Because continuous demographic variables and global network measures conformed to the normal distribution, a one-way analysis of variance (ANOVA) was performed to test whether significant between-group difference existed. If the test results indicated significant between-group differences, post hoc analyses were performed with the Tukey's honest significant difference method.

For all the statistical tests performed in this study, level of significance was set as 0.05.

2) Comparison of local network properties: connections and characteristics of nodes and edges

Because the brain connectivity data often do not conform to the normal distribution, permutation tests were performed for pair-wise comparison, yielding two-tailed raw p-values (Nichols and Holmes, 2002). Number of permutation was 20,000.

To correct a possible inflation of Type I errors arising from multiple tests for each set of measures, for which number of tests were from 82 (for nodes) to 3,221 (for edges), the false discovery rate (FDR) procedure were applied (Benjamini and

Hochberg, 1995). A FDR was set as 0.05 and adjusted p-values were yielded. Then the Bonferroni correction was used to adjust three pair-wise comparisons.

For any local network measures, both for nodes and edges, that were significantly different in a pair-wise comparison, I compared all three groups for that measures at a given node or edge as post hoc tests with raw p-values. Again, the Bonferroni correction was used to adjust three pair-wise comparisons. For any local measure that was different between groups, laterality indexes of that local measure were compared between groups with raw p-values to see a possible change in terms of hemispheric specialization.

To find edges that were different between groups, a core connection screening procedure was added before permutation tests (Duarte-Carvajalino et al., 2012; Zalesky et al., 2011). Because WM networks of the brain were sparsely connected and most of reconstructed edges were weak or non-existent, stringent multiple comparison correction procedure became unnecessarily stricter. For a core connection screening, we selected edges that were shared by more than 80% of NC subjects, which were 229 among 3,321 edges in this study, then performed statistical tests on those edges.

3) Correlation between network measures and clinical characterisitics

To find clinical meanings of network measures that were different between groups, Pearson's correlational analysis was performed between network and clinical measures.

4) Statistical software

All statistical tests were performed using Matlab R2012b Statistics Toolbox(TM) and in-house codes.

III. Results

1. Demographic and clinical characteristics of study participants

Age, sex, IQ, education years were not significantly different between groups (Table 1). The majority of study participants were right-handed and there was no significant difference in handedness between groups.

The UHR and FEP groups were not different in term of PANSS total, negative symptoms, and general psychopathology scores, and HAMD, and GAF scores. However, PANSS positive symptom scores, which reflects severity of positive symptoms of psychosis like delusion, hallucination, and hostility, were significantly higher in the FEP compared to the UHR group (t = -2.18, p = 0.033). The symptom severities of the FEP group were between mild to moderate because many of them were on antipsychotic treatment.

2. Comparison of gross constituents of networks

Intracranial volumes, total wiring lengths and total number of edges were not different between groups (Table 2). Although ANOVA indicated significant between-group difference in edge density (F = 3.295, p = 0.041), no group was

different from another at a post hoc test. This discrepancy may stem from sensitivity of ANOVA which detects slight difference of means. Taken together, a gross structural property and constituents of reconstructed networks of the brain were preserved in the UHR and FEP groups.

3. Global network properties

At the global level, global efficiency, characteristic path length, global clustering coefficient, and small-worldness were not different between groups (Table 2). However, modularity Q was higher in the UHR compared to the HC group ($F = 4.115$, $p = 0.019$) and assortativity coefficient was higher in the UHR compared to the FEP group ($F = 4.555$, $p = 0.013$).

4. Local network properties:connections and characteristics of nodes and edges

The connection strength between the left hippocampus and ipsilateral parahippocampal gyrus decreased in the FEP compared to the HC group (adjusted $p = 0.0115$; Figure 2 (a) and (b)). A *post hoc* analysis revealed that the connection also decreased in the FEP compared to the UHR group (raw $p = 0.0047$). A

Table 1. Demographic and clinical characteristics of study subjects

	HC (N = 37)		UHR (N = 37)		FEP (N=21)		Statistics	
	Mean	SD	Mean	SD	Mean	SD	*F*	*p*
Age	21.2	2.2	20.8	2.5	21.8	3.9	0.76	0.469
IQ	111.1	13.2	111.5	12.1	104.7	8.6	2.48	0.089
Education year	13.5	0.9	13.1	1.2	13.2	2	0.64	0.53
Intracranial volume (*l*)	1.57	0.16	1.57	0.12	1.59	0.17	0.14	0.87
							t	*p*
PANSS total			64.3	12.6	66.3	13.4	-0.55	0.583
Positive			13.3	2.9	15.6	5.1	-2.18	0.033*
Negative			17.3	5.3	16.3	5.6	0.65	0.519
General			33.8	7.7	34.4	6.8	-0.31	0.760
HAMD			12.5	5.8	9.5	5.3	1.94	0.058
GAF			48.8	6.6	49.2	11.9	-0.19	0.851
	n	%	n	%	n	%	X^2	*p*
Female	14	37.8	11	29.7	13	61.9	5.89	0.052
Left handedness	3	8.1	4	10.8	1	4.7	0.64	0.725

*$p < 0.05$

Table 2. Gross constituents of networks and global graph measures.

	HC (N = 37)		UHR (N = 37)		FEP (N = 21)		Statistics		
	Mean	SD	Mean	SD	Mean	SD	*F*	*p*	*Post hoc*
Gross Constituents of networks									
Total wiring length (*m*)	118	18	112	17	121	23	1.721	0.185	
Total number of edges	6406	509	6276	635	6229	714	0.700	0.499	
Edge density	0.109	0.005	0.106	0.006	0.109	0.006	3.295	0.041*	ns
Global network measures									
Measures of integration									
Characteristic path length	46.19	4.71	46.8	5.34	45.6	6.8	0.335	0.716	
Global efficiency	0.032	0.003	0.032	0.003	0.032	0.004	0.197	0.821	
Measures of segregation									
Global clustering coefficient	0.035	0.007	0.036	0.006	0.037	0.006	0.699	0.500	
Modularity Q	0.584	0.014	0.594	0.017	0.587	0.016	4.115	0.019*	UHR > HC
A measure of resilience									
Assortativity coefficient	0.101	0.050	0.116	0.042	0.078	0.044	4.555	0.013*	UHR > FEP
Other									
Small-worldness	4.375	0.334	4.437	0.291	4.543	0.276	2.018	0.139	

*$p < 0.05$

connection between the left thalamus and ipsilateral superior frontal gyrus increased in the FEP compared to the HC group (adjusted $p = 0.0115$; Figure 2 (c) and (d)). A *post hoc* analysis revealed that the connection increased in the FEP compared to the UHR group (raw $p = 0.0006$). Although the laterality index of the connections between both thalami and ipsilateral superior frontal gyri was not different between groups, the laterality index of the connections between both hippocampi and ipsilateral parahippocampal gyri was significantly different. The FEP group showed more rightward laterality of the latter connections than the HC and UHR groups ($p = 0.0064$ and 0.0086; Figure 3 (a) and (b)).

For characteristics of nodes, only participation coefficient showed significant between-group difference. The participation coefficient of the right pallidum increased in the FEP compared to the HC group (adjusted $p = 0.0041$; Figure 4 (a)). A *post hoc* analysis revealed that the measure also increased in the FEP compared to the UHR group (raw $p = 0.0112$). The laterality index of the participation coefficients of both pallida was not significantly different between groups.

Centrality measures of nodes were only marginally altered. Strength of the left hippocampus decreased in the FEP compared to the HC group and degree of the right thalamus decreased in the UHR compared to the HC group at a trend level (adjusted $p = 0.0205$ and 0.0287). Within-module degree z, node betweenness, clustering coefficient and local efficiency were not different between groups (see supplementary table in the Appendix for summary of statistical tests of local graph measures and supplementary figures for distribution of p values for local network measures).

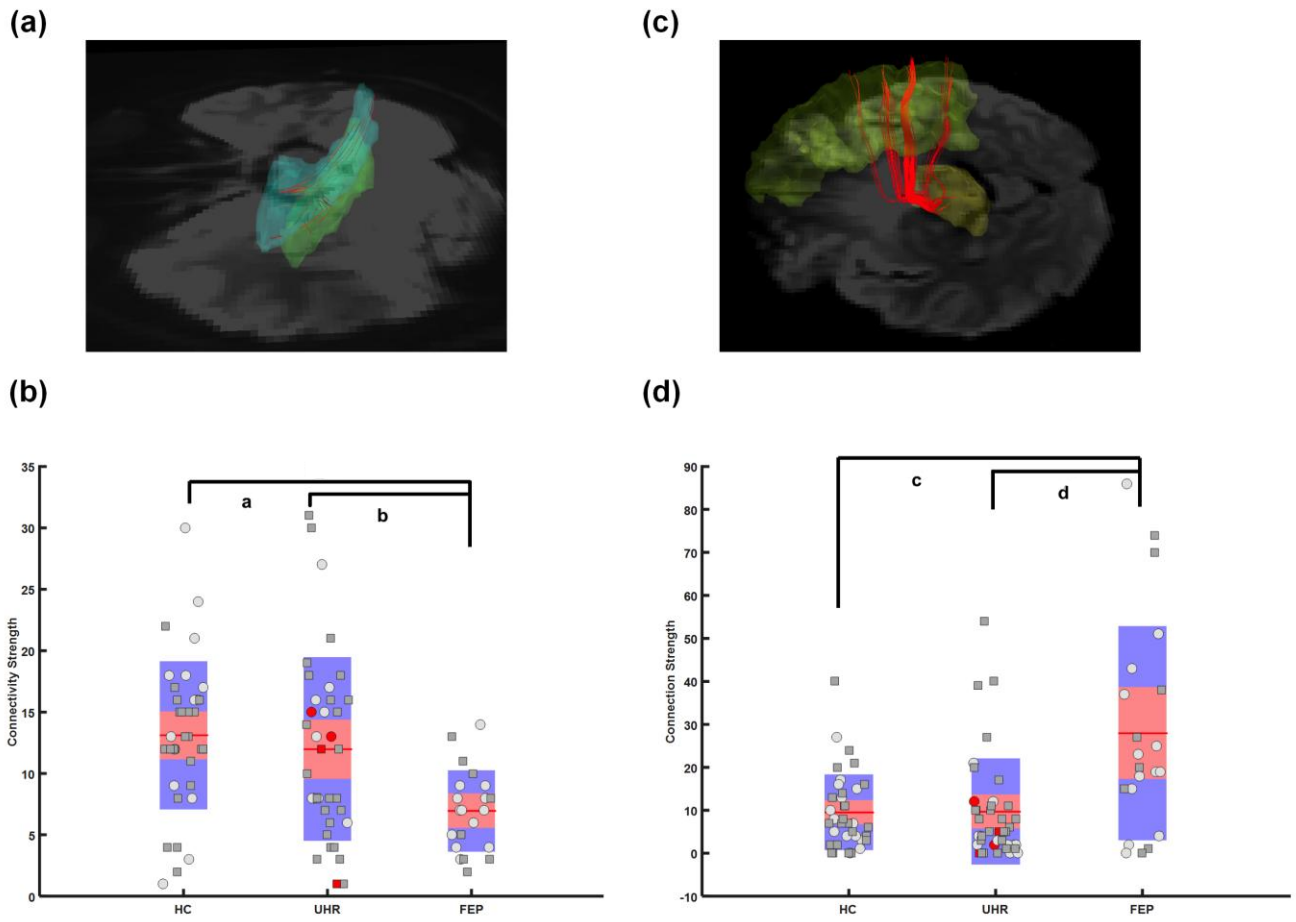
(a)
(c)
(b)
(d)
Connectivity Strength
Connection Strength
a
b
c
d
HC
UHR
FEP

Figure 2. The connection strengths between (a),(b) the left hippocampus (sky blue) and ipsilateral parahippocampal gyrus (green), and (c),(d) the left thalamus (olive) and ipsilateral superior frontal gyrus (lime). The red lines are interconnecting fibers. Squares and circles indicate male and female subjects, and red-filled ones indicate those who converted to psychosis ((c) and (d)).

[a] adjusted $p = 0.0015$; [b] raw $p = 0.0047$ (*post hoc* test); [c] adjusted $p = 0.0015$; [d] raw $p = 0.0006$ (*post hoc* test).

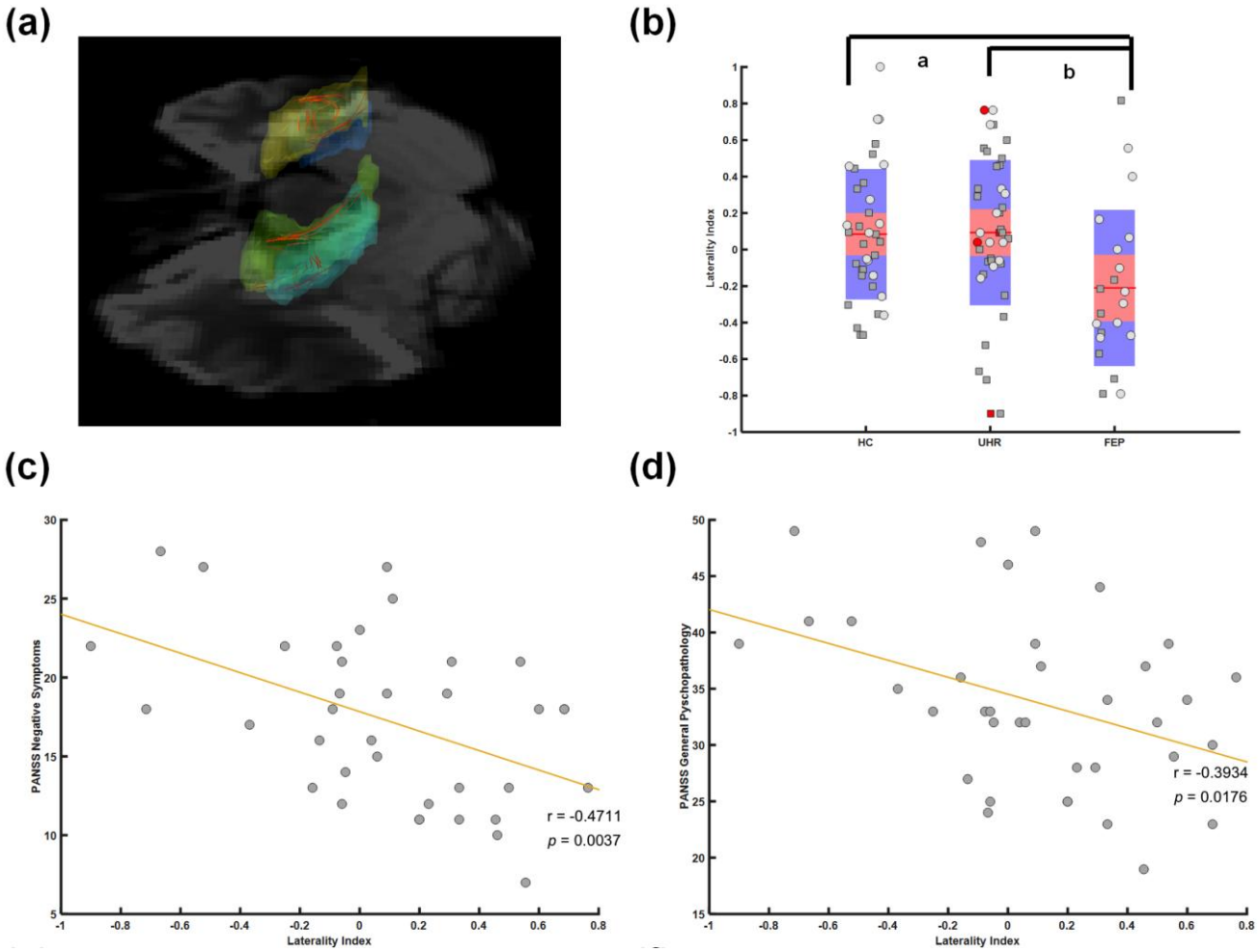
(a)
(b)
a
b
Laterality Index
HC
UHR
FEP
(c)
PANSS Negative Symptoms
Laterality Index
r = -0.4711
p = 0.0037
(d)
PANSS General Pyschopathology
Laterality Index
r = -0.3934
p = 0.0176

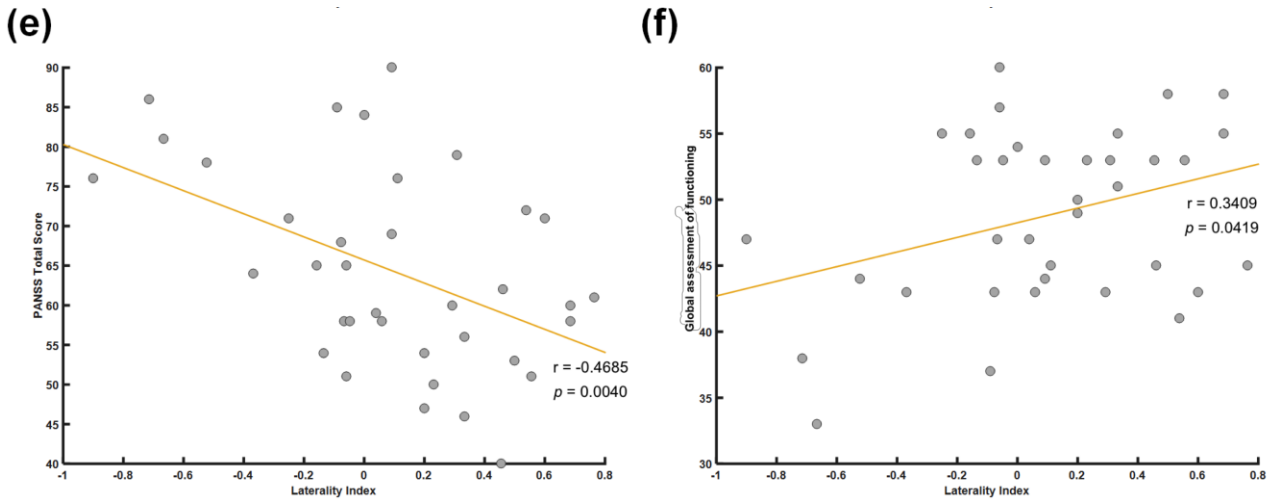

Figure 3. (a),(b) The laterality index of connection strengths between both hippocampi (left:green , right:yellow) and ipsilateral parahippocampal gyri (left:turquoise, right:blue). The red lines are interconnecting fibers. The UHR group showed correlations between the laterality index and (c) PANSS negative symptoms, (d) PANSS general psychopathology and (e) PANSS total scores, and (f) global assessment of functioning score. Squares and circles indicate male and female subjects, and red-filled ones indicate those who converted to psychosis (b).

[a]p = 0.0064; [b]p=0.0086

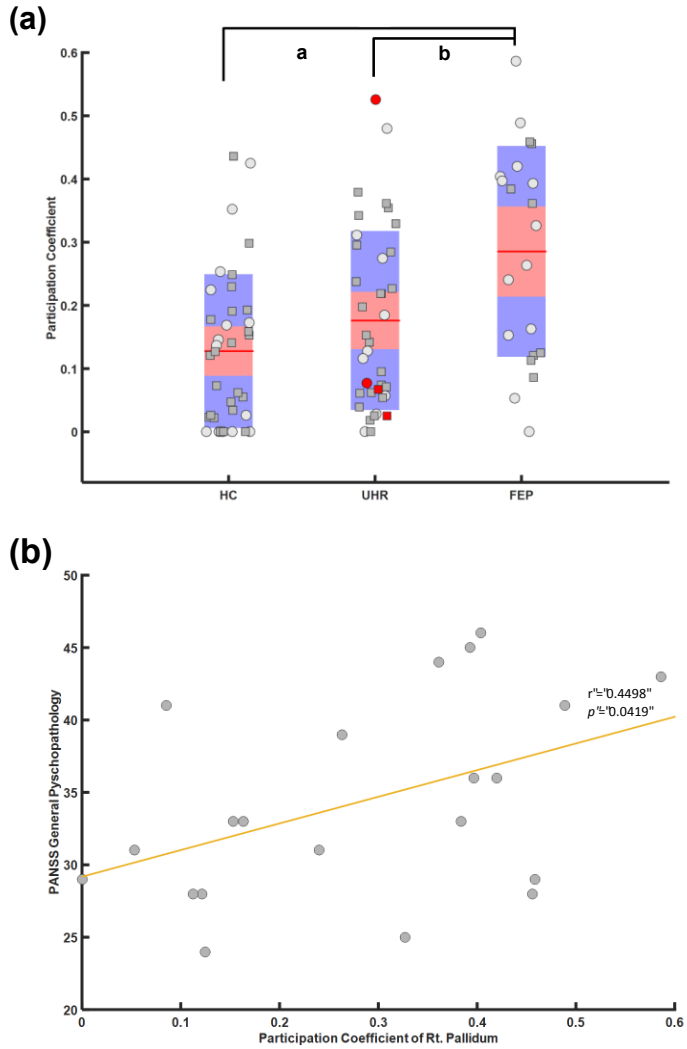

Figure 4. (a) The participation coefficient of the right pallidum and (b) its correlation with the PANSS general psychopathology score in the FEP group. Squares and circles indicate male and female subjects, and red-filled ones indicate those who converted to psychosis (a).

[a] adjusted $p = 0.0041$;[b] raw $p = 0.0112$ (*post hoc* test)

For characteristics of edges, edge betweenness and shortest path length did not differ between groups.

5. Correlation between aberrant network characteristics and clinical measures

The laterality index of the connections between both hippocampi and ipsilateral parahippocampal gyri correlated negatively with the PANSS negative symptoms, general psychopathology, and total scores, and positively with the GAF score in the UHR group (r = -0.4711, p = 0.0037; r = -0.3934, p = 0.0176; r = -0.4685, p = 0.0040; r = 0.3409, p = 0.0419; respectively; Figure 3 (c) ~ (f)). In the FEP group, the participation coefficient of the right pallidum positively correlated with the PANSS general psychopathology score (r = 0.4498, p = 0.0408; Figure 4 (b)). Other measures that were significantly different between groups did not show a correlation with clinical variables.

IV. Discussion

In this study, I showed that both global and local network characteristics retrieved from reconstructed axonal brain network were differentially altered in subjects with UHR and FEP. This is the first study that investigated graph characteristics of WM brain network of UHR, and compared UHR with FEP simultaneously to see whether differential changes would exist according to the different stages of psychosis. The results indicate that alteration of the WM network of the brain in UHR and FEP might be subtle. UHR differed from FEP and HC only in global network characteristics and FEP was disrupted mainly in cortico-subcortical connectivity.

1. Altered global graph characteristics in UHR

At the global level, degree of integration of the WM brain network as measured by global efficiency was not altered in UHR and FEP. Among measures reflecting degree of segregation, degree of modularity increased in the UHR compared to the HC group although global clustering coefficient was not different between groups. Although both global clustering coefficient and modularity Q can be classified as a measure of segregation, each measure reflects a different aspect of clustering. Global clustering coefficient represents how well neighbors of a node are connected,

thus sometimes called as ‘local efficiency’ (Achard et al., 2006; Latora and Marchiori, 2001) (Note that this ‘local efficiency’ is different from the local efficiency described in the method section which is a node-specific local network characteristic). On the other hand, modularity *Q* represents how well a given separation into modules within a network performs. Networks with high modularity have dense connections within a module and sparse connections between modules and vice versa. Biological networks tend to have high modularity (Kaiser, 2011). Taken together, while global efficiency and degree of clustering of networks were not altered, degree of modularity increased in UHR. Modular structure is regarded as a key driver of evolution of a biological organism because it is cost-effective in terms of maximizing performance while reducing connection costs (Clune et al., 2013). In this regard, by increasing modularity, the brain of UHR might try to enhance its functions without altering connection cost, to defend against further deterioration of the brain network which might lead to conversion into psychosis.

Assortative mixing of nodes was higher in the UHR than FEP groups. A network with high assortitivity coefficient has highly interconnected high-degree hubs that make the network resilient to a possible damage to a hub (Rubinov and Sporns, 2010). At the same time, a network with high assortativity tends to easily transmit information or spread a disease via interconnected high-degree hubs (Newman, 2002). Possible explanation is that, by increasing assortativity of the network, the compensatory brain connectivity in UHR may prepare for further damage to the network, which might occur during progression into a more severe illness. Alternatively, higher assortativity in UHR may partly explain attenuated

psychotic symptoms that can be understood as a result of under-optimized filtering and easily transmitting of redundant information within the network.

On the other hand, I could not find disrupted small-world network properties reflected by small-worldness in the UHR and FEP group. Disrupted small-world property in schizophrenia is one of the frequently replicated findings in graph theoretical analysis across imaging modalities (Jalili and Knyazeva, 2011; Liu et al., 2008; Lynall et al., 2010;Ma et al., 2012; Micheloyannis et al., 2006; Rubinov et al., 2009; Wang et al., 2012; Zalesky et al., 2011). However, preserved small-worldness in schizophrenia was observed from DTI (van den Heuvel et al., 2010), cortical-thickness correlation (Bassett et al., 2008), and task-related fMRI (Fornito et al., 2011) studies, too.

In contrast to our findings, previous studies also found decreased modularity (Alexander-Bloch et al., 2010; Jalili and Knyazeva, 2011), decreased assortativity (Jalili and Knyazeva, 2011), increased characteristic path length (Liu et al., 2008), decreased global clustering coefficient (Alexander-Bloch et al., 2010; He et al., 2012; Lynall et al., 2010) and decreased average nodal degree (Zalesky et al., 2011) in schizophrenia, although findings are not consistent across studies.

Interestingly, one study from patients with first-episode schizophrenia with task-related fMRI found that all major global graph characteristics such as small-worldness, global and local efficiencies, characteristic path length and global clustering coefficient were preserved (Fornito et al., 2011) as in this study. A recent DTI study also reported preserved small-world property in the medication-naive schizophrenia patients (Zhang et al., 2015). On the other hand, the DTI study

reported decreased global efficiency of the network, and increased characteristic path length along with decreased network strength which is the mean of nodal strengths, and network degree which is the mean of nodal degree. However, sparsity of a network, which is reflected by the network degree and strength, could affect a degree of integration. Sparse network tends to have lower integration and clustering (Kaiser, 2011). Being the network of the first-episode schizophrenia sparse, it was hard to distinguish whether those changes might be attributable to the changes of individual characteristics per se or rather to network sparsity. On the other hand, results from the present study did not indicate alteration in network sparsity, that was reflected by preserved total counts of streamlines (network strength multiplied by the total number of nodes) and edge density in the UHR and FEP groups. The difference in the network sparsity of FEP in the present study and of first-episode schizophrenia may partly stem from medication-status of study participants, although studies on effects of antipsychotic medications to the WM integrity produced mixed results (Bartzokis et al., 2007; Szeszko et al., 2014). Taken together, I suppose that the reported changes of the previous DTI study may be attributable rather to sparse network of the first-episode schizophrenia.

In summary, alterations of global organizational properties of networks may not simply depend on whether one could be diagnosed as having schizophrenia or not. Rather they may depend on different stages and duration of the illness. Although global network characteristics of FEP was not different from HC, those of UHR was so from HC or FEP in the direction of increasing resilience and function the network without altering connection costs. A gradual change along with progression

into psychosis was not found. Rather, UHR may be a unique state distinguishable from both HC and FEP in terms of global network properties.

2. Altered local graph characteristics in FEP

The weaker connection between the left hippocampus and ipsilateral parahippocampal gyrus in FEP may reflect abnormalities in the hippocampal formation, the core structure in declarative memory. It includes the hippocampus, the entorhinal cortex, the dentate gyrus, and the parahippocampal gyrus (Ranganath and Ritchey, 2012), and is considered as a key structure in pathophysiology of schizophrenia (Weinberger, 1999). Impairment of visual and verbal declarative memory is consistent findings in schizophrenia along with impairment of other cognitive functions such as working memory and processing speeds (Tamminga et al., 2010). A study reported that lower performance in verbal memory task identified UHR subjects who would later develop into psychosis (Brewer et al., 2005).

Abnormality of the hippocampus is a consistent finding in schizophrenia research in terms of both structure and function and both macro- and micro-scales (Tamminga et al., 2010). Reduction of bilateral hippocampal volumes or only in the left side is evident even in the first episode patients (Buehlmann et al., 2010; Phillips et al., 2002; Velakoulis et al., 2006; Witthaus et al., 2010). Moreover most studies on UHR subjects who later developed into psychosis indicate smaller

hippocampal volumes than controls (Francis et al., 2013; Mittal et al., 2013; Moorhead et al., 2013; Wood et al., 2010).

Parahippocampal hypoactivation during a declarative memory task was found among patients with schizophrenia and their healthy siblings and parahippocampal activation was positively correlated with task performance (Rasetti et al., 2014). Other studies reported aberrant activations in the parahippocampal gyrus during emotional tasks (Escarti et al., 2010; Kang et al., 2009). Decreased volume of the parahippocampal gyrus was also found in patients with schizophrenia along with that of the hippocampus in structural MRI (Sim et al., 2006) and postmortem studies (Bogerts et al., 1985; Brown et al., 1986). Disrupted WM structure in the left parahippocampal gyrus was also reported in childhood-onset schizophrenia (Serene et al., 2007). In this regard, decreased connection strength between the left hippocampus and adjacent parahippocampal gyrus in the FEP group in this study might indicate alteration in the circuit of the hippocampal formation, especially in the left side.

Interestingly, the change on asymmetry in the connections between both hippocampi and ipsilateral parahippocampal gyri not only was found in the FEP group, but also correlated with several clinical variables in the UHR group, which indicates that the change is biologically relevant. Crow et al. (1989) suggested that schizophrenia results from a failure of normal cerebral lateralization. Several neuroimaging studies revealed abnormal lateralization pattern in the brain of patients with schizophrenia (Oertel-Knochel and Linden, 2011)

The connection strength between the left thalamus and ipsilateral superior

frontal gyrus decreased in the FEP group in this study. Abnormalities in the thalamocortical network in schizophrenia are suggested as primary or secondary to interconnected cortical and subcortical pathology. They may be neural correlates underlying abnormal tuning of thought process by failure of ensembles of cortical and thalamic neural oscillations (Jones, 1997). Especially, the thalamo-prefrontal resting-state functional connectivity is largely absent until adolescence, and develop during transition to adulthood in children and adolescents (Fair et al., 2010). Because the timing of maturation of the thalamo-prefrontal connection coincides with the timing of typical psychotic breakdown, disruption in maturation of the connection could be a candidate of neurodevelopmental mechanism underlying developmental process of psychosis.

A study that explored distinct thalamocortical WM connectivity according to cortical ROIs in schizophrenia showed reduced connection between the thalamus and the lateral prefrontal cortex in schizophrenia. However, it is unclear whether there is a unilateral change in the thalamo-prefrontal connectivity because the study treated the same cortical ROIs from both hemispheres as one (Marenco et al., 2012). Moreover, because it used relative connectivity in relation with total thalamocortical connectivity, it is hard to compare the study finding directly with mine, in which absolute number of WM streamlines count. On the other hand, resting-state functional imaging studies on the thalamocortical connectivity also reported decrease in the left thalamo-prefrontal connection (Woodward et al., 2012) and in the connection between thalamus and the left superior frontal gyrus (Wang et al., 2015). The left superior frontal gyrus is implicated in introspective function of self

(Goldberg et al., 2006), and an fMRI study reported hypoactivation in the region during self-appraisal task in schizophrenia (Bedford et al., 2012). Self-appraisal includes insights being ill and impaired reality testing is one of core features of psychosis. Thalamocortical loop was proposed as a neural basis of consciousness (Llinas et al., 1998), which may be closely related to self-appraisal. Self-appraisal is rather a complex process that may require feedback loops between the regions and mainly the thalamus, within which fine-tuning of information could occur. Taken together, increased connectivity between those two regions in the present study may result from abnormally faster maturation of the interconnecting WM fibers and reflect aberrant self-appraisal in first-episode psychosis, although the reason why the finding from the previous functional study has the opposite direction of change from mine remains to be explored.

Along with these findings, participation coefficient, degree of connection beyond its participating module of a node (Guimera and Amaral, 2005), in the right pallidum was increased in FEP than UHR and HC. If a participation coefficient of a node is high, the node tends to exert more effects beyond the participating module and, conversely, less within that module. Increased participation coefficient of that region in the FEP group may reflect altered modular structure within basal ganglia. Interestingly, an increase in this measure is positively correlated with degree of general psychopathology in the FEP group, thus indicating that altered modular property of the right pallidum might be an underlying neurobiological basis of psychiatric symptoms in FEP.

All local alterations evident in the FEP group, except for the laterality index of

both hippocampi and ipsilateral parahippocampal gyri, were observed in the UHR groups in a lesser extent although the alterations were not statistically significant. These findings may reflect that UHR has similarities with FEP in terms not only of symptom phenomenology but also of local network properties.

In contrast to previous studies on schizophrenia, the present study did not find widely distributed local connectomic changes in FEP. As mentioned earlier, the discrepancy might stem from different phases of the illness across studies. Previous studies on structural and functional properties of the brain consistently showed less extensive abnormalities in the first-episode and prodromal phase of schizophrenia (Peters et al., 2010). Notably, findings on chronic schizophrenia could be confounded by lots of factors such as prolonged exposure to drugs, social isolation, and degenerative process of the illness that could affect the brain. Likewise, alteration in graph measures might not be extensive in these early stages of the illness.

3. Limitations

This study suffers from several limitations. Because this study was not a longitudinal but cross-sectional one, true progressive changes along with psychosis-continuum could not directly be traced. A relatively small sample size could have limited statistical power of the study. Lack of a region-specific hypothesis, which might lessen number of tests, may have further limited power of this study.

A possible influence of sex dimorphism on study findings might be a concern because proportion of women in the FEP group was, albeit not significant, slightly higher than the UHR and, much less extent, HC groups. However, I could not find a direct influence of ratios of women on the measures that were significantly different between groups. If sex ratios were a major factor influencing the results, I should have found results indicating FEP the highest, UHR the lowest, and HC in the middle, or vice versa. Moreover, previous studies on sexual dimorphism do not commonly indicate differences in the limbic region (Gong et al., 2011) or bilateral rather symmetric changes (Chou et al., 2011). Visualization of sex in the Figures did not indicate possible influence of sex on the study results.

On the other hand, the present study has several strengths. By comparing UHR, FEP and HC concurrently, differential changes in the WM connectivity along with different stages of psychosis could be reliably investigated. This study also included important subcortical structures in network reconstruction and, in turn, detected significant changes mainly in the cortico-subcortical connectivity. Unlike many studies that rely on functional correlations in reconstructing brain network, this study utilized diffusion tensor imaging method which enables direct investigation into the WM fiber connectivity that is stable and independent of task-conditions. Finally, because the high resolution 3-Tesla diffusion tensor imaging has better imaging resolution compared to the traditional 1.5-Tesla one, more refined fiber-tracking was possible in this study.

V. Conclusion

In this study, I showed that UHR is a unique stage that enhances resilience and adaptability of the WM network that may reflect highly variable prognosis of the stage among psychosis-continuum on the one hand, and defensive mechanism against further damage on the network on the other. The main alteration on the WM network of FEP mainly lies in the cortico-subcortical connectivity. These differential changes may reflect underlying biological mechanisms of developmental process leading to psychosis. Future longitudinal studies will elucidate structural and functional network alterations during development into psychosis. Comprehensive understanding of the brain dysconnectivity, underlying schizophrenia or psychosis in general, could hopefully lead to the development of specific targeted interventions that could halt or restore alteration in the brain connectivity of individuals with UHR.

VI. References

1. Achard, S., Bullmore, E., 2007. Efficiency and cost of economical brain functional networks. PLoS Comput Biol 3, e17.

2. Achard, S., Salvador, R., Whitcher, B., Suckling, J., Bullmore, E., 2006. A resilient, low-frequency, small-world human brain functional network with highly connected association cortical hubs. J Neurosci 26, 63-72.

3. Adriano, F., Spoletini, I., Caltagirone, C., Spalletta, G., 2010. Updated meta-analyses reveal thalamus volume reduction in patients with first-episode and chronic schizophrenia. Schizophr Res 123, 1-14.

4. Alexander-Bloch, A.F., Gogtay, N., Meunier, D., Birn, R., Clasen, L., Lalonde, F., Lenroot, R., Giedd, J., Bullmore, E.T., 2010. Disrupted modularity and local connectivity of brain functional networks in childhood-onset schizophrenia. Front Syst Neurosci 4, 147.

5. Barrat, A., Barthelemy, M., Pastor-Satorras, R., Vespignani, A., 2004. The architecture of complex weighted networks. Proc Natl Acad Sci U S A 101, 3747-3752.

6. Bartzokis, G., Lu, P.H., Nuechterlein, K.H., Gitlin, M., Doi, C., Edwards, N., Lieu, C., Altshuler, L.L., Mintz, J., 2007. Differential effects of typical

and atypical antipsychotics on brain myelination in schizophrenia. Schizophr Res 93, 13-22.

7. Bassett, D.S., Bullmore, E., 2006. Small-world brain networks. Neuroscientist 12, 512-523.

8. Bassett, D.S., Bullmore, E., Verchinski, B.A., Mattay, V.S., Weinberger, D.R., Meyer-Lindenberg, A., 2008. Hierarchical organization of human cortical networks in health and schizophrenia. J Neurosci 28, 9239-9248.

9. Bedford, N.J., Surguladze, S., Giampietro, V., Brammer, M.J., David, A.S., 2012. Self-evaluation in schizophrenia: an fMRI study with implications for the understanding of insight. BMC Psychiatry 12, 106.

10. Benjamini, Y., Hochberg, Y., 1995. Controlling the false discovery rate: a practical and powerful approach to multiple testing. J Roy Stat Soc Ser B (Stat Method), 289-300.

11. Bogerts, B., Meertz, E., Schonfeldt-Bausch, R., 1985. Basal ganglia and limbic system pathology in schizophrenia. A morphometric study of brain volume and shrinkage. Arch Gen Psychiatry 42, 784-791.

12. Bolanos, M., Bernat, E.M., He, B., Aviyente, S., 2013. A weighted small world network measure for assessing functional connectivity. J Neurosci Methods 212, 133-142.

13. Brandes, U., 2001. A faster algorithm for betweenness centrality. J Math Sociol 25, 163-177.

14. Brewer, W.J., Francey, S.M., Wood, S.J., Jackson, H.J., Pantelis, C., Phillips, L.J., Yung, A.R., Anderson, V.A., McGorry, P.D., 2005. Memory impairments identified in people at ultra-high risk for psychosis who later develop first-episode psychosis. Am J Psychiatry 162, 71-78.

15. Brown, R., Colter, N., Corsellis, J.A., Crow, T.J., Frith, C.D., Jagoe, R., Johnstone, E.C., Marsh, L., 1986. Postmortem evidence of structural brain changes in schizophrenia. Differences in brain weight, temporal horn area, and parahippocampal gyrus compared with affective disorder. Arch Gen Psychiatry 43, 36-42.

16. Buehlmann, E., Berger, G.E., Aston, J., Gschwandtner, U., Pflueger, M.O., Borgwardt, S.J., Radue, E.W., Riecher-Rossler, A., 2010. Hippocampus abnormalities in at risk mental states for psychosis? A cross-sectional high resolution region of interest magnetic resonance imaging study. J Psychiatr Res 44, 447-453.

17. Cao, Q., Shu, N., An, L., Wang, P., Sun, L., Xia, M.R., Wang, J.H., Gong, G.L., Zang, Y.F., Wang, Y.F., He, Y., 2013. Probabilistic diffusion tractography and graph theory analysis reveal abnormal white matter structural connectivity networks in drug-naive boys with attention deficit/hyperactivity disorder. J Neurosci 33, 10676-10687.

18. Chou, K.H., Cheng, Y., Chen, I.Y., Lin, C.P., Chu, W.C., 2011. Sex-linked white matter microstructure of the social and analytic brain. NeuroImage 54, 725-733.

19. Clune, J., Mouret, J.B., Lipson, H., 2013. The evolutionary origins of modularity. Proc Biol Sci 280.

20. Crow, T.J., Ball, J., Bloom, S.R., Brown, R., Bruton, C.J., Colter, N., Frith, C.D., Johnstone, E.C., Owens, D.G., Roberts, G.W., 1989. Schizophrenia as an anomaly of development of cerebral asymmetry. A postmortem study and a proposal concerning the genetic basis of the disease. Arch Gen Psychiatry 46, 1145-1150.

21. Danon, L., Diaz-Guilera, A., Duch, J., Arenas, A., 2005. Comparing community structure identification. J Stat Mech 2005, P09008.

22. Desikan, R.S., Segonne, F., Fischl, B., Quinn, B.T., Dickerson, B.C., Blacker, D., Buckner, R.L., Dale, A.M., Maguire, R.P., Hyman, B.T., Albert, M.S., Killiany, R.J., 2006. An automated labeling system for subdividing the human cerebral cortex on MRI scans into gyral based regions of interest. NeuroImage 31, 968-980.

23. Duarte-Carvajalino, J.M., Jahanshad, N., Lenglet, C., McMahon, K.L., de Zubicaray, G.I., Martin, N.G., Wright, M.J., Thompson, P.M., Sapiro, G., 2012. Hierarchical topological network analysis of anatomical human brain

connectivity and differences related to sex and kinship. NeuroImage 59, 3784-3804.

24. Escarti, M.J., de la Iglesia-Vaya, M., Marti-Bonmati, L., Robles, M., Carbonell, J., Lull, J.J., Garcia-Marti, G., Manjon, J.V., Aguilar, E.J., Aleman, A., Sanjuan, J., 2010. Increased amygdala and parahippocampal gyrus activation in schizophrenic patients with auditory hallucinations: an fMRI study using independent component analysis. Schizophr Res 117, 31-41.

25. Fair, D.A., Bathula, D., Mills, K.L., Dias, T.G., Blythe, M.S., Zhang, D., Snyder, A.Z., Raichle, M.E., Stevens, A.A., Nigg, J.T., Nagel, B.J., 2010. Maturing thalamocortical functional connectivity across development. Front Syst Neurosci 4, 10.

26. First, M., Spitzer, R., Gibbon, M., Williams, J., 1995. Structured Clinical Interview for DSM-IV Axis I Disorders, Non-Patient Edition (SCID-NP). Biometrics Research Department, New York State Psychiatric Institute, New York.

27. Fischl, B., Salat, D.H., Busa, E., Albert, M., Dieterich, M., Haselgrove, C., van der Kouwe, A., Killiany, R., Kennedy, D., Klaveness, S., Montillo, A., Makris, N., Rosen, B., Dale, A.M., 2002. Whole brain segmentation: automated labeling of neuroanatomical structures in the human brain. Neuron 33, 341-355.

28. Fischl, B., van der Kouwe, A., Destrieux, C., Halgren, E., Segonne, F., Salat, D.H., Busa, E., Seidman, L.J., Goldstein, J., Kennedy, D., Caviness, V., Makris, N., Rosen, B., Dale, A.M., 2004. Automatically parcellating the human cerebral cortex. Cereb Cortex 14, 11-22.

29. Fornito, A., Yoon, J., Zalesky, A., Bullmore, E.T., Carter, C.S., 2011. General and specific functional connectivity disturbances in first-episode schizophrenia during cognitive control performance. Biol Psychiatry 70, 64-72.

30. Francis, A.N., Seidman, L.J., Tandon, N., Shenton, M.E., Thermenos, H.W., Mesholam-Gately, R.I., van Elst, L.T., Tuschen-Caffier, B., DeLisi, L.E., Keshavan, M.S., 2013. Reduced subicular subdivisions of the hippocampal formation and verbal declarative memory impairments in young relatives at risk for schizophrenia. Schizophr Res 151, 154-157.

31. Fusar-Poli, P., Borgwardt, S., Bechdolf, A., Addington, J., Riecher-Rossler, A., Schultze-Lutter, F., Keshavan, M., Wood, S., Ruhrmann, S., Seidman, L.J., Valmaggia, L., Cannon, T., Velthorst, E., De Haan, L., Cornblatt, B., Bonoldi, I., Birchwood, M., McGlashan, T., Carpenter, W., McGorry, P., Klosterkotter, J., McGuire, P., Yung, A., 2013. The psychosis high-risk state: a comprehensive state-of-the-art review. JAMA Psychiatry 70, 107-120.

32. Girvan, M., Newman, M.E., 2002. Community structure in social and biological networks. Proc Natl Acad Sci U S A 99, 7821-7826.

33. Goldberg, II, Harel, M., Malach, R., 2006. When the brain loses its self: prefrontal inactivation during sensorimotor processing. Neuron 50, 329-339.

34. Gong, G., He, Y., Evans, A.C., 2011. Brain connectivity: gender makes a difference. Neuroscientist 17, 575-591.

35. Guimera, R., Amaral, L.A., 2005. Cartography of complex networks: modules and universal roles. J Stat Mech 2005, nihpa35573.

36. Hamilton, M., 1960. A rating scale for depression. J Neurol Neurosurg Psychiatry 23, 56-62.

37. He, H., Sui, J., Yu, Q., Turner, J.A., Ho, B.C., Sponheim, S.R., Manoach, D.S., Clark, V.P., Calhoun, V.D., 2012. Altered small-world brain networks in schizophrenia patients during working memory performance. PLoS One 7, e38195.

38. Humphries, M.D., Gurney, K., 2008. Network 'small-world-ness': a quantitative method for determining canonical network equivalence. PLoS One 3, e0002051.

39. Jalili, M., Knyazeva, M.G., 2011. EEG-based functional networks in schizophrenia. Comput Biol Med 41, 1178-1186.

40. Jones, E.G., 1997. Cortical development and thalamic pathology in schizophrenia. Schizophr Bull 23, 483-501.

41. Jung, M.H., Jang, J.H., Kang, D.H., Choi, J.S., Shin, N.Y., Kim, H.S., An, S.K., Shin, M.S., Kwon, J.S., 2010. The reliability and validity of the Korean version of the structured interview for prodromal syndrome. Psychiatry Investig 7, 257-263.

42. Jung, W.H., Kim, J.S., Jang, J.H., Choi, J.S., Jung, M.H., Park, J.Y., Han, J.Y., Choi, C.H., Kang, D.H., Chung, C.K., Kwon, J.S., 2011. Cortical thickness reduction in individuals at ultra-high-risk for psychosis. Schizophr Bull 37, 839-849.

43. Kaiser, M., 2011. A Tutorial in Connectome Analysis: Topological and Spatial Features of Brain Networks. NeuroImage 57, 892-907.

44. Kang, J.I., Kim, J.J., Seok, J.H., Chun, J.W., Lee, S.K., Park, H.J., 2009. Abnormal brain response during the auditory emotional processing in schizophrenic patients with chronic auditory hallucinations. Schizophr Res 107, 83-91.

45. Kay, S.R., Fiszbein, A., Opler, L.A., 1987. The positive and negative syndrome scale (PANSS) for schizophrenia. Schizophr Bull 13, 261-276.

46. Korgaonkar, M.S., Fornito, A., Williams, L.M., Grieve, S.M., 2014. Abnormal structural networks characterize major depressive disorder: a connectome analysis. Biol Psychiatry 76, 567-574.

47. Kwon, J.S., Shim, G., Park, H.Y., Jang, J.H., 2010. Current concept of prodrome from the experience of the Seoul Youth Clinic High Risk Cohort in Korea. Clin Neuropsychiatry 7, 56-62.

48. Latora, V., Marchiori, M., 2001. Efficient behavior of small-world networks. Phys Rev Lett 87, 198701.

49. Leung, C., Chau, H., 2007. Weighted assortative and disassortative networks model. Physica A 378, 591-602.

50. Liu, Y., Liang, M., Zhou, Y., He, Y., Hao, Y., Song, M., Yu, C., Liu, H., Liu, Z., Jiang, T., 2008. Disrupted small-world networks in schizophrenia. Brain 131, 945-961.

51. Llinas, R., Ribary, U., Contreras, D., Pedroarena, C., 1998. The neuronal basis for consciousness. Philos Trans R Soc Lond B Biol Sci 353, 1841-1849.

52. Lynall, M.E., Bassett, D.S., Kerwin, R., McKenna, P.J., Kitzbichler, M., Muller, U., Bullmore, E., 2010. Functional connectivity and brain networks in schizophrenia. J Neurosci 30, 9477-9487.

53. Ma, S., Calhoun, V.D., Eichele, T., Du, W., Adali, T., 2012. Modulations of functional connectivity in the healthy and schizophrenia groups during task and rest. NeuroImage 62, 1694-1704.

54. Marenco, S., Stein, J.L., Savostyanova, A.A., Sambataro, F., Tan, H.Y., Goldman, A.L., Verchinski, B.A., Barnett, A.S., Dickinson, D., Apud, J.A., Callicott, J.H., Meyer-Lindenberg, A., Weinberger, D.R., 2012. Investigation of anatomical thalamo-cortical connectivity and FMRI activation in schizophrenia. Neuropsychopharmacology 37, 499-507.

55. Micheloyannis, S., Pachou, E., Stam, C.J., Breakspear, M., Bitsios, P., Vourkas, M., Erimaki, S., Zervakis, M., 2006. Small-world networks and disturbed functional connectivity in schizophrenia. Schizophr Res 87, 60-66.

56. Miller, T.J., McGlashan, T.H., Rosen, J.L., Cadenhead, K., Cannon, T., Ventura, J., McFarlane, W., Perkins, D.O., Pearlson, G.D., Woods, S.W., 2003. Prodromal assessment with the structured interview for prodromal syndromes and the scale of prodromal symptoms: predictive validity, interrater reliability, and training to reliability. Schizophr Bull 29, 703-715.

57. Miller, T.J., McGlashan, T.H., Rosen, J.L., Somjee, L., Markovich, P.J., Stein, K., Woods, S.W., 2002. Prospective diagnosis of the initial prodrome for schizophrenia based on the Structured Interview for Prodromal Syndromes: preliminary evidence of interrater reliability and predictive validity. Am J Psychiatry 159, 863-865.

58. Mittal, V.A., Gupta, T., Orr, J.M., Pelletier-Baldelli, A., Dean, D.J., Lunsford-Avery, J.R., Smith, A.K., Robustelli, B.L., Leopold, D.R.,

Millman, Z.B., 2013. Physical activity level and medial temporal health in youth at ultra high-risk for psychosis. J Abnorm Psychol 122, 1101-1110.

59. Moorhead, T.W., Stanfield, A.C., McKechanie, A.G., Dauvermann, M.R., Johnstone, E.C., Lawrie, S.M., Cunningham Owens, D.G., 2013. Longitudinal gray matter change in young people who are at enhanced risk of schizophrenia due to intellectual impairment. Biol Psychiatry 73, 985-992.

60. Mori, S., Barker, P.B., 1999. Diffusion magnetic resonance imaging: its principle and applications. Anat Rec 257, 102-109.

61. Newman, M.E., 2002. Assortative mixing in networks. Phys Rev Lett 89, 208701.

62. Newman, M.E., 2004. Fast algorithm for detecting community structure in networks. Phys Rev E Stat Nonlin Soft Matter Phys 69, 066133.

63. Nichols, T.E., Holmes, A.P., 2002. Nonparametric permutation tests for functional neuroimaging: a primer with examples. Hum Brain Mapp 15, 1-25.

64. Oertel-Knochel, V., Linden, D.E.J., 2011. Cerebral Asymmetry in Schizophrenia. Neuroscientist 17, 456-467.

65. Onnela, J.-P., Saramäki, J., Kertész, J., Kaski, K., 2005. Intensity and coherence of motifs in weighted complex networks. Physical Review E 71.

66. Peters, B.D., Blaas, J., de Haan, L., 2010. Diffusion tensor imaging in the early phase of schizophrenia: What have we learned? J Psychiatr Res 44, 993-1004.

67. Phillips, L.J., Velakoulis, D., Pantelis, C., Wood, S., Yuen, H.P., Yung, A.R., Desmond, P., Brewer, W., McGorry, P.D., 2002. Non-reduction in hippocampal volume is associated with higher risk of psychosis. Schizophr Res 58, 145-158.

68. Ranganath, C., Ritchey, M., 2012. Two cortical systems for memory-guided behaviour. Nat Rev Neurosci 13, 713-726.

69. Rasetti, R., Mattay, V.S., White, M.G., Sambataro, F., Podell, J.E., Zoltick, B., Chen, Q., Berman, K.F., Callicott, J.H., Weinberger, D.R., 2014. Altered hippocampal-parahippocampal function during stimulus encoding: a potential indicator of genetic liability for schizophrenia. JAMA Psychiatry 71, 236-247.

70. Rubinov, M., Knock, S.A., Stam, C.J., Micheloyannis, S., Harris, A.W., Williams, L.M., Breakspear, M., 2009. Small-world properties of nonlinear brain activity in schizophrenia. Hum Brain Mapp 30, 403-416.

71. Rubinov, M., Sporns, O., 2010. Complex network measures of brain connectivity: Uses and interpretations. NeuroImage 52, 1059-1069.

72. Rubinov, M., Sporns, O., 2011. Weight-conserving characterization of complex functional brain networks. NeuroImage 56, 2068-2079.

73. Rudie, J.D., Brown, J.A., Beck-Pancer, D., Hernandez, L.M., Dennis, E.L., Thompson, P.M., Bookheimer, S.Y., Dapretto, M., 2012. Altered functional and structural brain network organization in autism. Neuroimage Clin 2, 79-94.

74. Sanz-Arigita, E.J., Schoonheim, M.M., Damoiseaux, J.S., Rombouts, S.A., Maris, E., Barkhof, F., Scheltens, P., Stam, C.J., 2010. Loss of 'small-world' networks in Alzheimer's disease: graph analysis of FMRI resting-state functional connectivity. PLoS One 5, e13788.

75. Serene, J.A., Ashtari, M., Szeszko, P.R., Kumra, S., 2007. Neuroimaging studies of children with serious emotional disturbances: a selective review. Can J Psychiatry 52, 135-145.

76. Shin, K.S., Kim, J.S., Kang, D.H., Koh, Y., Choi, J.S., O'Donnell, B.F., Chung, C.K., Kwon, J.S., 2009. Pre-attentive auditory processing in ultra-high-risk for schizophrenia with magnetoencephalography. Biol Psychiatry 65, 1071-1078.

77. Sim, K., DeWitt, I., Ditman, T., Zalesak, M., Greenhouse, I., Goff, D., Weiss, A.P., Heckers, S., 2006. Hippocampal and parahippocampal volumes in schizophrenia: a structural MRI study. Schizophr Bull 32, 332-340.

78. Supekar, K., Menon, V., Rubin, D., Musen, M., Greicius, M.D., 2008. Network analysis of intrinsic functional brain connectivity in Alzheimer's disease. PLoS Comput Biol 4, e1000100.

79. Szeszko, P.R., Robinson, D.G., Ikuta, T., Peters, B.D., Gallego, J.A., Kane, J., Malhotra, A.K., 2014. White matter changes associated with antipsychotic treatment in first-episode psychosis. Neuropsychopharmacology 39, 1324-1331.

80. Tamminga, C.A., Stan, A.D., Wagner, A.D., 2010. The hippocampal formation in schizophrenia. Am J Psychiatry 167, 1178-1193.

81. van den Heuvel, M.P., Mandl, R.C., Stam, C.J., Kahn, R.S., Hulshoff Pol, H.E., 2010. Aberrant frontal and temporal complex network structure in schizophrenia: a graph theoretical analysis. J Neurosci 30, 15915-15926.

82. van Os, J., Kapur, S., 2009. Schizophrenia. Lancet 374, 635-645.

83. Velakoulis, D., Wood, S.J., Wong, M.T., McGorry, P.D., Yung, A., Phillips, L., Smith, D., Brewer, W., Proffitt, T., Desmond, P., Pantelis, C., 2006. Hippocampal and amygdala volumes according to psychosis stage and diagnosis: a magnetic resonance imaging study of chronic schizophrenia, first-episode psychosis, and ultra-high-risk individuals. Arch Gen Psychiatry 63, 139-149.

84. Wang, H.L., Rau, C.L., Li, Y.M., Chen, Y.P., Yu, R., 2015. Disrupted thalamic resting-state functional networks in schizophrenia. Front Behav Neurosci 9, 45.

85. Wang, Q., Su, T.P., Zhou, Y., Chou, K.H., Chen, I.Y., Jiang, T., Lin, C.P., 2012. Anatomical insights into disrupted small-world networks in schizophrenia. NeuroImage 59, 1085-1093.

86. Wang, R., Benner, T., Sorensen, A.G., Wedeen, V.J., 2007. Diffusion Toolkit: A Software Package for Diffusion Imaging Data Processing and Tractography. Proc Intl Soc Mag Reson Med 15, No. 3720.

87. Watts, D.J., 1999. Small worlds: the dynamics of networks between order and randomness. Princeton university press.

88. Watts, D.J., Strogatz, S.H., 1998. Collective dynamics of 'small-world' networks. Nature 393, 440-442.

89. Weinberger, D.R., 1999. Cell biology of the hippocampal formation in schizophrenia. Biol Psychiatry 45, 395-402.

90. Witthaus, H., Mendes, U., Brune, M., Ozgurdal, S., Bohner, G., Gudlowski, Y., Kalus, P., Andreasen, N., Heinz, A., Klingebiel, R., Juckel, G., 2010. Hippocampal subdivision and amygdalar volumes in patients in an at-risk mental state for schizophrenia. J Psychiatry Neurosci 35, 33-40.

91. Wood, S.J., Kennedy, D., Phillips, L.J., Seal, M.L., Yucel, M., Nelson, B., Yung, A.R., Jackson, G., McGorry, P.D., Velakoulis, D., Pantelis, C., 2010. Hippocampal pathology in individuals at ultra-high risk for psychosis: a multi-modal magnetic resonance study. NeuroImage 52, 62-68.

92. Woodward, N.D., Karbasforoushan, H., Heckers, S., 2012. Thalamocortical dysconnectivity in schizophrenia. Am J Psychiatry 169, 1092-1099.

93. Yi, J.S., Ahn, Y.M., Shin, H.K., An, S.K., Joo, Y.H., Kim, S.H., Yoon, D.J., Jho, K.H., Koo, Y.J., Lee, J.Y., 2001. Reliability and validity of the Korean version of the Positive and Negative Syndrome Scale. J Korean Neuropsychiatr Assoc 40, 1090-1105.

94. Yung, A.R., McGorry, P.D., McFarlane, C.A., Jackson, H.J., Patton, G.C., Rakkar, A., 1996. Monitoring and care of young people at incipient risk of psychosis. Schizophr Bull 22, 283-303.

95. Yung, A.R., Phillips, L.J., Yuen, H.P., McGorry, P.D., 2004. Risk factors for psychosis in an ultra high-risk group: psychopathology and clinical features. Schizophr Res 67, 131-142.

96. Zalesky, A., Fornito, A., Seal, M.L., Cocchi, L., Westin, C.F., Bullmore, E.T., Egan, G.F., Pantelis, C., 2011. Disrupted axonal fiber connectivity in schizophrenia. Biol Psychiatry 69, 80-89.

97. Zhang, J., Wang, J., Wu, Q., Kuang, W., Huang, X., He, Y., Gong, Q., 2011. Disrupted brain connectivity networks in drug-naive, first-episode major depressive disorder. Biol Psychiatry 70, 334-342.

98. Zhang, R., Wei, Q., Kang, Z., Zalesky, A., Li, M., Xu, Y., Li, L., Wang, J., Zheng, L., Wang, B., Zhao, J., Zhang, J., Huang, R., 2015. Disrupted brain anatomical connectivity in medication-naive patients with first-episode schizophrenia. Brain Struct Funct 220, 1145-1159.

VII. Appendix

Supplementary material. List of ROIs

Frontal ROIs

Superior Frontal

Rostral and Caudal Middle Frontal

Pars Opercularis, Pars Triangularis, and Pars Orbitalis

Lateral and Medial Orbitofrontal

Precentral

Paracentral

Frontal Pole

Parietal ROIs

Superior Parietal

Inferior Parietal

Supramarginal

Postcentral

Precuneus

Temporal ROIs

Superior, Middle, and Inferior Temporal

Banks of the Superior Temporal Sulcus

Fusiform

Transverse Temporal

Entorhinal

Temporal Pole

Parahippocampal

Occipital ROIs

Lateral Occipital

Lingual

Cuneus

Pericalcarine

Cingulate ROIs

Rostral Anterior

Caudal Anterior

Posterior

Isthmus

Others (including subcortical structures)

Insula

Thalamus

Caudate

Putamen

Pallidum

Hippocampus

Amygdala

Nucleus Accumbens

Supplementary table. Summary of statistical tests and brief accounts for each graph measure.

Measures	Tests (n)	Findings (n)	Brief accouts
Global	1		
Gross			
Total wiring length		0	Sum of (edge weights x track length)
Total number of edges		0	Sum of edge weights
Edge density		0	Proportion of existing connections within a network
Integration			
Characteristic path length		0	Mean of shortest path lengths (see edge-based measures)
Global efficiency		0	Mean of 1/(shortest path length)
Segregation			
Global clustering coefficient		0	Mean of clustering coefficient (see node-based measures)
Modularity *Q*		1	How clearly a network could be divided by delineated groups
Resilience			
Assortativity coefficient		1	How resilient a network against targeted attack to hubs
Other			
Small-worldness		0	The characteristic of a network that is both highly clustered and efficient because of the presence of long-range connections between clusters
Connection strengths	229	2	Number of WM streamlines

Measures	Tests (n)	Findings (n)	
Node-based	82		
Centrality			
Degree		0	How many nodes are connected
Strength		0	How many streamlines are connected
Node betweenness		0	How many shortest paths pass through
Regional clustering			
Clustering coefficient		0	How densely connected between neighboring nodes.
Modular properties			
Participation coefficient		1	How densely connected beyond the participating module.
Within-module degree *z*		0	How densely connected within the participating module.
Other			
Local efficiency		0	How easily a signal could be transferred within the subgraph containing the node
Edge-based	3321		
Edge betweenness		0	How many shortest paths pass through
Shortest path length		0	the shortest distance between two nodes
Laterality indexes	3	1	Hemisphreric Asymmetry of seemingly symmetrical structures

Note: Comparison of laterality indexes is contingent on significant local findings. For global measures see Table 1.

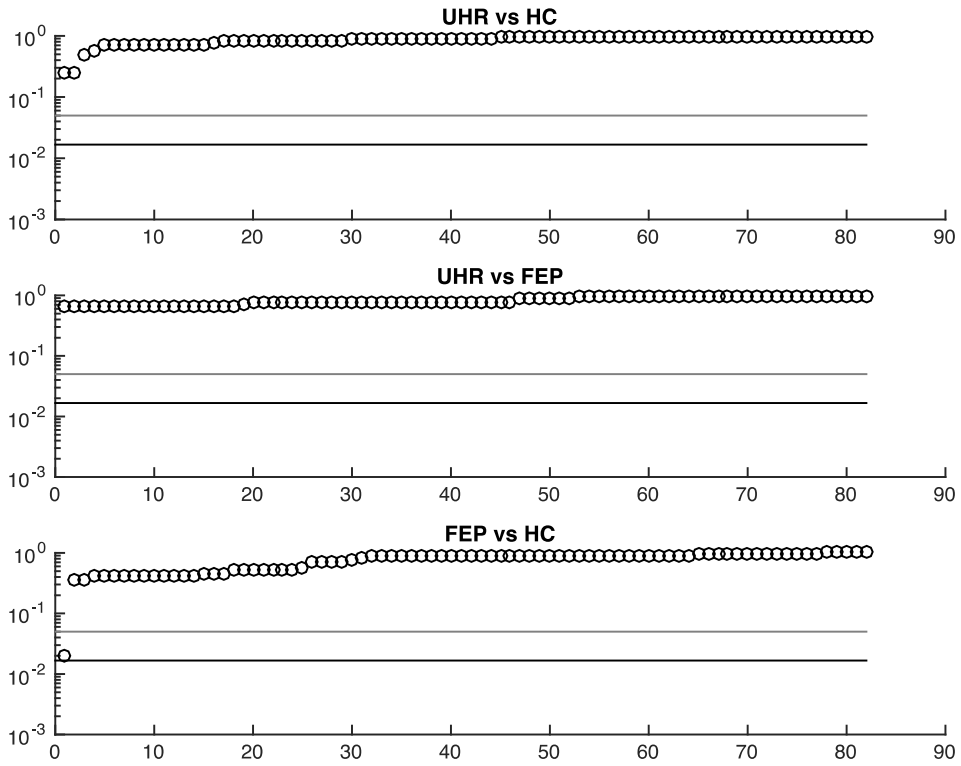

Figure S1. Distribution of adjusted p-values for nodal strength. The black line indicates the Bonferroni-corrected threshold (p = 0.0167) and the grey line indicates 0.05. The node between the two lines (FEP vs HC) is the left hippocampus.

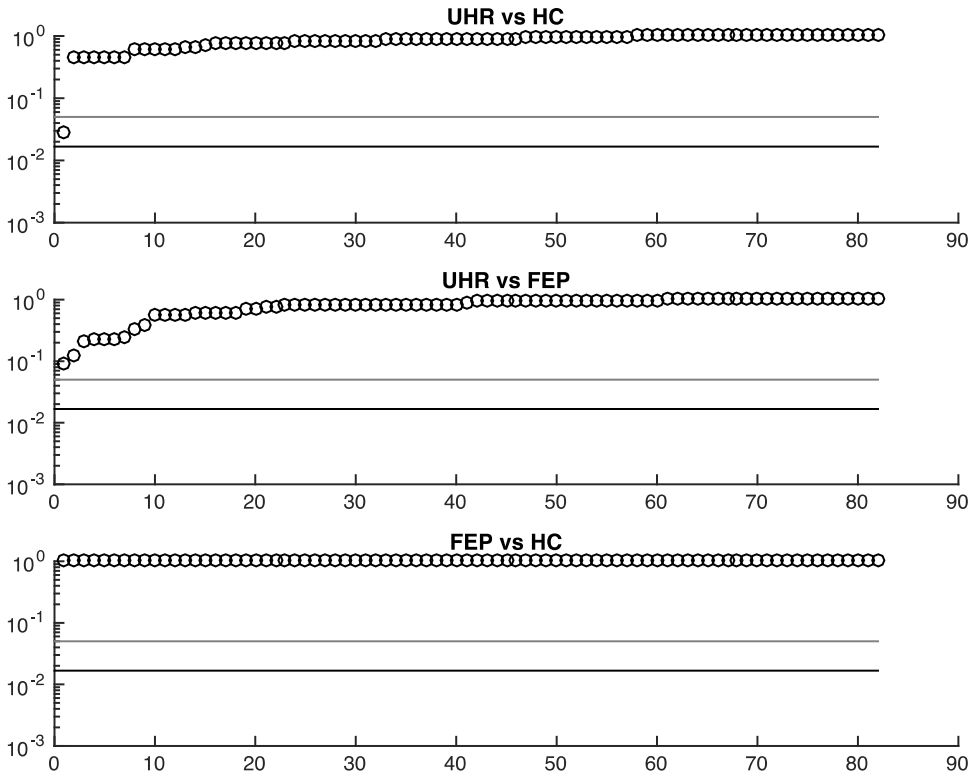

Figure S2. Distribution of adjusted p-values for nodal degree. The black and grey lines indicate the Bonferroni-corrected threshold (p = 0.0167) and 0.05. The node between the two lines (UHR vs HC) is the right thalamus.

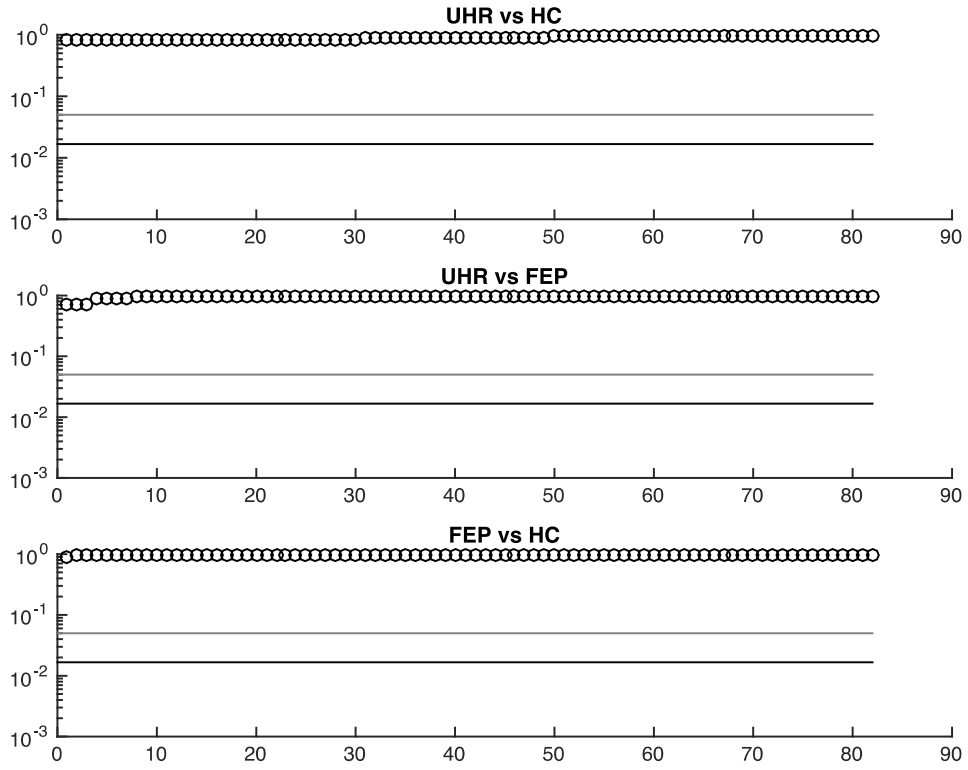

Figure S3. Distribution of adjusted p-values for clustering coefficient of nodes. The black and grey lines indicate the Bonferroni-corrected threshold (p = 0.0167) and 0.05.

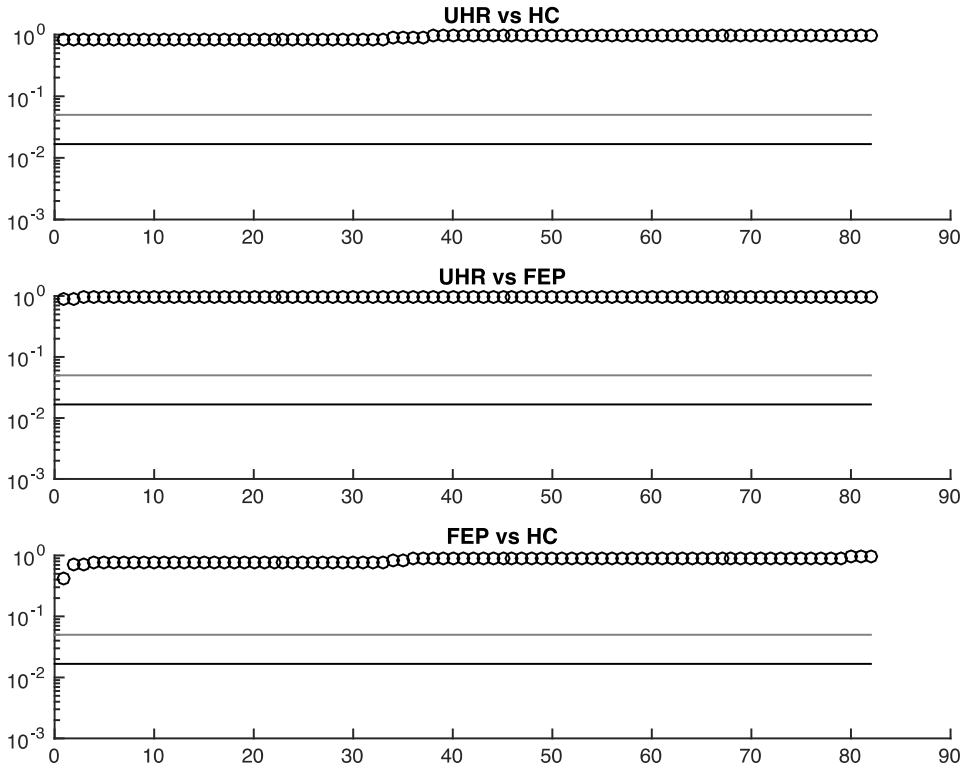

Figure S4. Distribution of adjusted p-values for local efficiency of the subgraph of a node. The black and grey lines indicate the Bonferroni-corrected threshold (p = 0.0167) and 0.05.

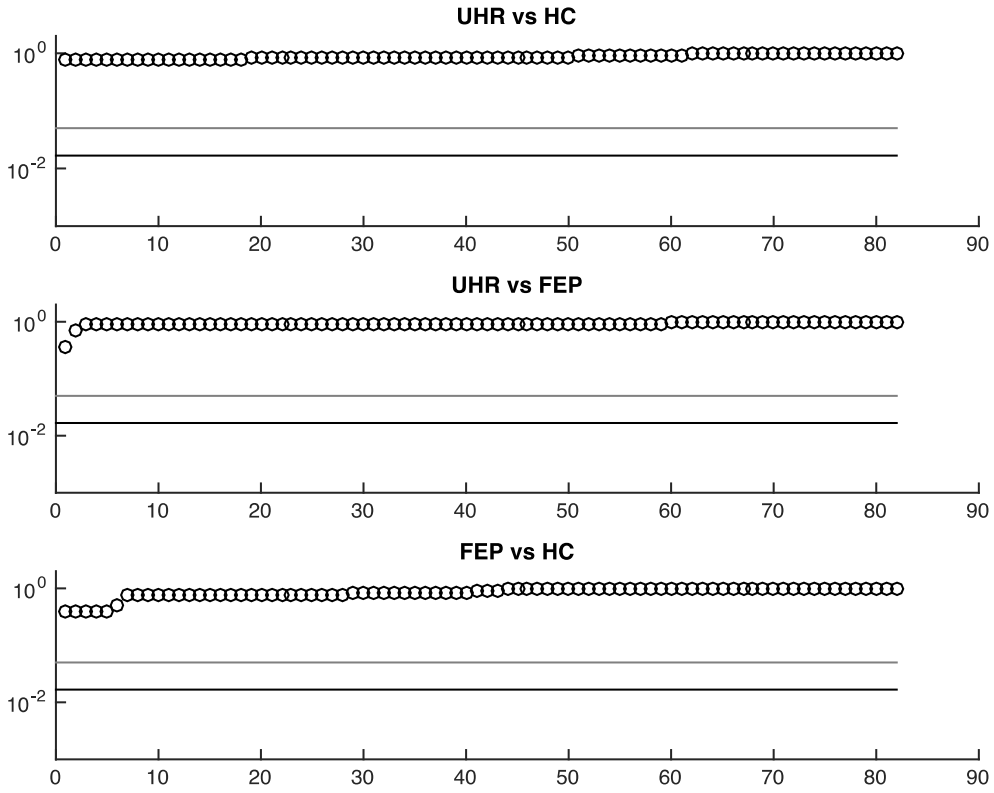

Figure S5. Distribution of adjusted p-values for node betweenness. The black and grey lines indicate the Bonferroni-corrected threshold (p = 0.0167) and 0.05.

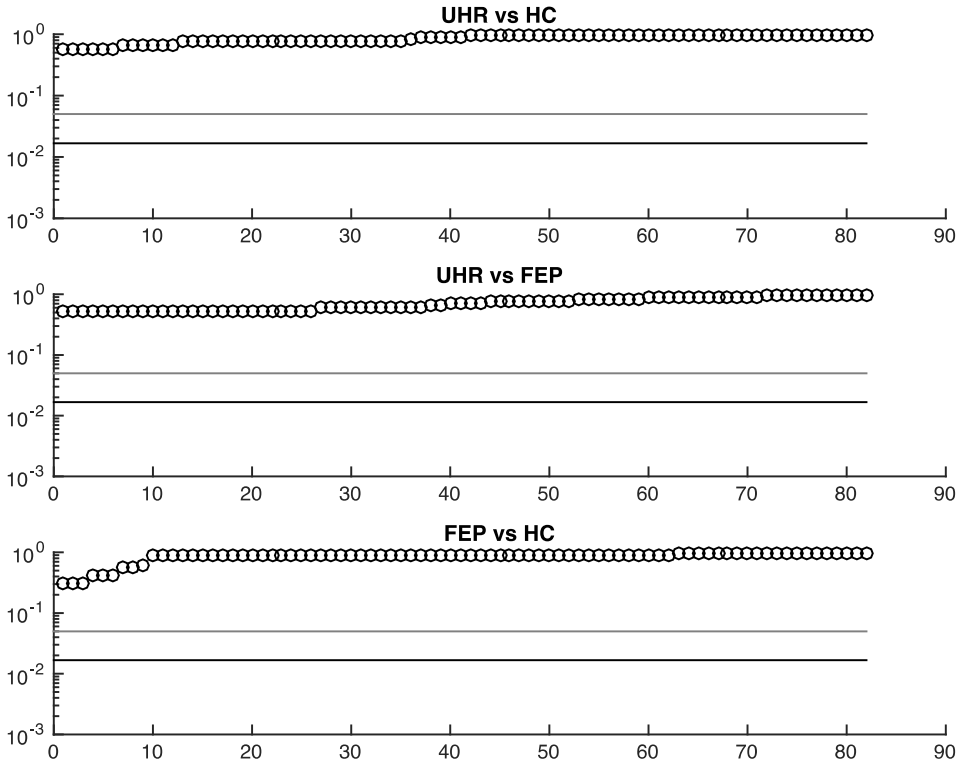

Figure S6. Distribution of adjusted p-values for within-module degree *z*. The black and grey lines indicate the Bonferroni-corrected threshold (p = 0.0167) and 0.05.

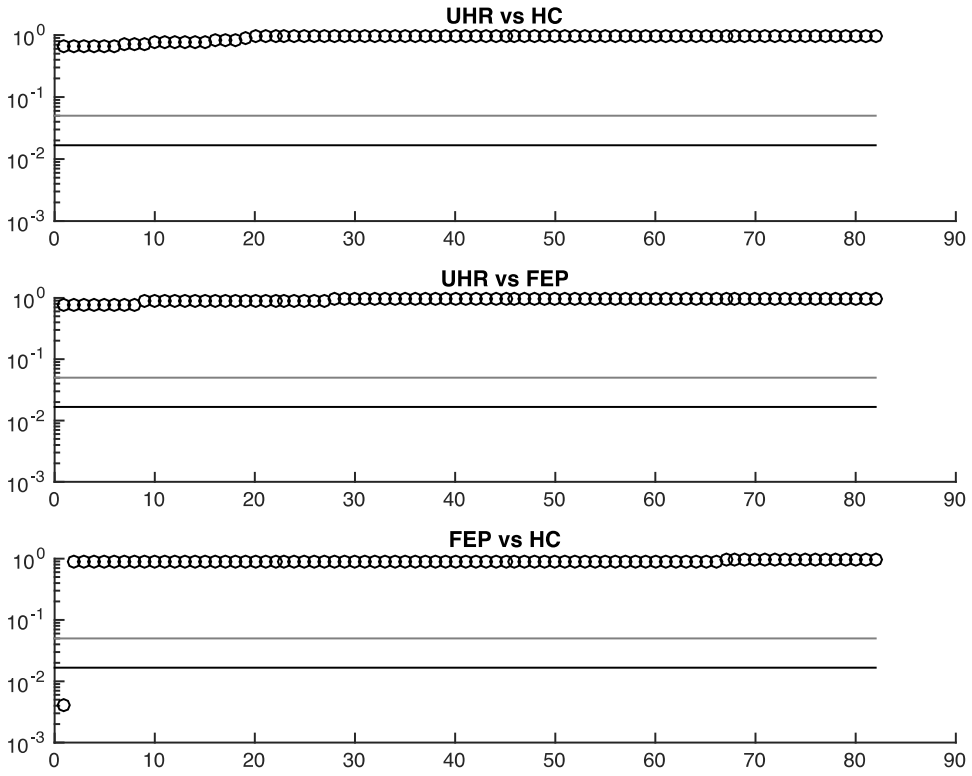

Figure S7. Distribution of adjusted p-values for participation coefficient of a node. The black and grey lines indicate the Bonferroni-corrected threshold (p = 0.0167) and 0.05. The node below the black line (FEP vs HC) is the right pallidum.

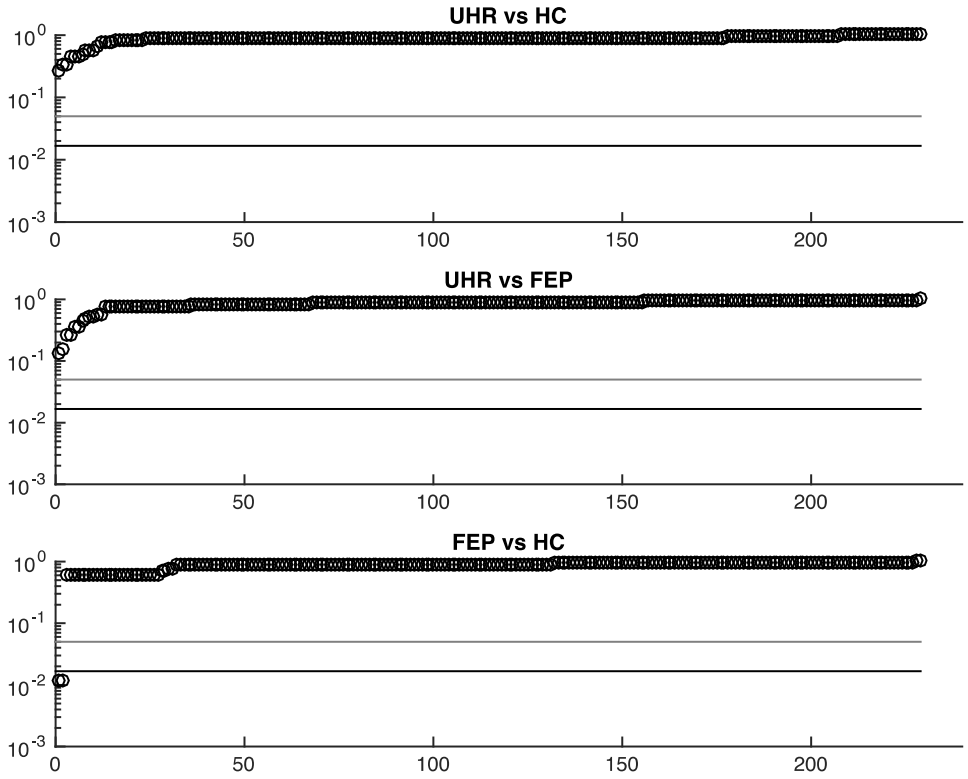

Figure S8. Distribution of adjusted p-values for the core connections between pairs of nodes. The black and grey lines indicate the Bonferroni-corrected threshold (p = 0.0167) and 0.05. The two nodes below the black line (FEP vs HC) are the connections between the left hippocampus and ipsilateral parahippocampal gyrus, and the left thalamus and ipsilateral superior frontal gyrus.

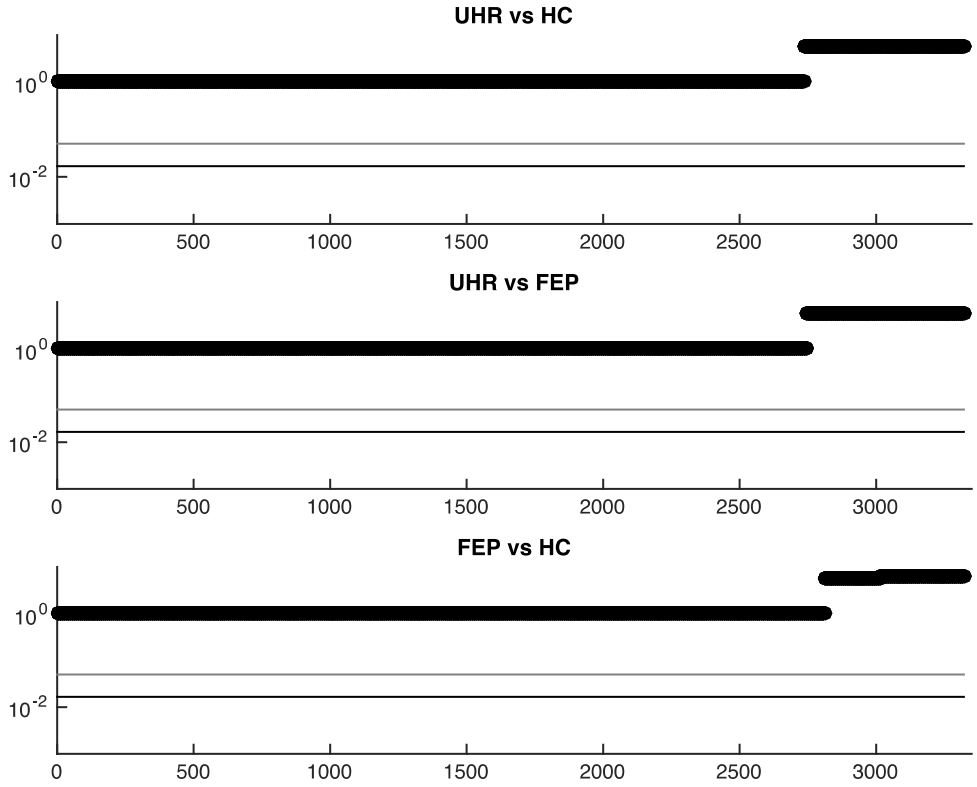

Figure S9. Distribution of adjusted p-values for edge betweenness. The black and grey lines indicate the Bonferroni-corrected threshold (p = 0.0167) and 0.05. Note that adjusted p-values yielded by the false-discovery rate (FDR) method could be greater than 1.

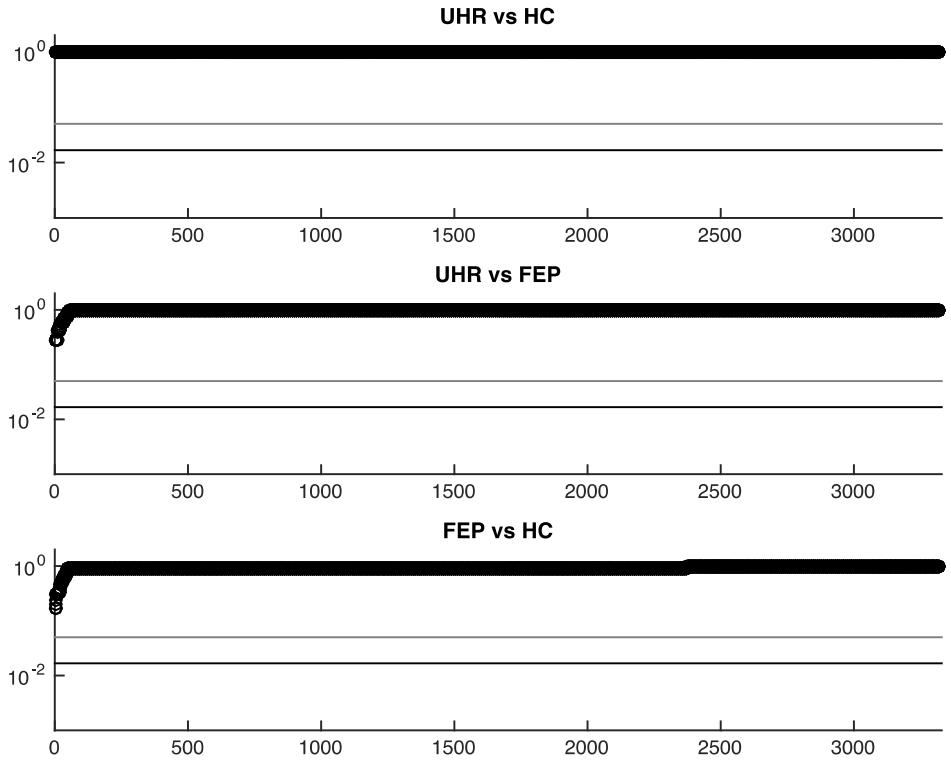

Figure S10. Distribution of adjusted p-values for the shortest path length between pairs of nodes. The black and grey lines indicate the Bonferroni-corrected threshold ($p = 0.0167$) and 0.05.

국문초록

조현병의 뇌 이상연결성을 통합적으로 이해하기 위해서는 네트워크 차원의 분석이 요구된다. 이 방법은 국소적 연결성 이상 뿐 아니라, 네트워크의 거시적 특성도 드러내기 때문이다. 그러나 아직까지 초발정신병 환자와 정신증 초고위험군에서 뇌 백질 네트워크의 이상을 비교 분석한 연구는 없었는데, 이러한 비교는 정신증으로 이행하는 데 따르는 차등적인 뇌의 해부학적 네트워크의 변화를 추적하는 데에 중요한 의미를 지닌다.

본 연구에는 37 명의 정신증 초고위험군 대상자와 21 명의 초발정신병 환자, 37 명의 건강한 대조군이 참여하였다. 3-Tesla T1 구조 영상과 확산텐서영상으로부터, 82 개의 피질과 피질하 영역을 점으로 하고 신경섬유다발 흐름의 수를 점을 연결하는 가중치를 갖는 선으로 하여 구성된 네트워크를 추출하였다. 그리고 이렇게 재구성된 네트워크로부터 계산된 그래프 특성을 군간 비교하였다.

네트워크의 통합성이나 작은 세상 네트워크 특성(small-worldness)을 반영하는 지표에서는 세 군간에 차이를 보이지 않았지만, 정신증 초고위험군에서는 동류상관계수(assrotativity coefficienct)가 초발정신병군에 비해 높았으며 모듈화 정도가 건강한 대조군에 비해 높았다. 전체집단화계수(global clustering coefficient)는 차이가 없었다. 국소적으로는 초발정신병군에서 건강한 대조군과 정신증 초고위험군에 비하여 좌측 해마와 동측 부해마회를 잇는 백질의 연결 강도가 감소한 반면, 좌측 시상과 동측 상전두회를 잇는 백질의 연결 강도는 증가하였다. 정신증 초고위험군와 건강한 대조군에 비하여 초발정신병 군에서 양측 해마와 동측 부해마회를 잇는 백질 연결 강도의 비대칭성이 우편향된 소견이 관찰되었으며, 정신증 초고위험군에서 우측 편측성의 정도가 정신증 증상과 양의 상관관계를, 기능 수준과는 음의 상관관계를 보였다. 우측 창백핵의 모듈참여지수(participation coefficient)는 초발정신병군에서 정신증 초고위험군과 건강한 대조군에 비하여 증가하였다. 초발정신병군에서 우측 창백핵의 모듈참여지수가 높을수록 비특이적인 정신증상이 심하였다.

정신증 초고위험군은 백질 네트워크의 적응탄력성과 적응성을 증가시키는 방향으로의 변화를 수반하는데, 이러한 변화는 이 단계의 다양한 예후를 반영하면서, 정신증으로 이행할 시에 가해질 네트위크의 손상에 대비하는

기전으로 생각된다. 반면에, 초발정신병에서는 주로 피질-피질하 연결성에서의 국소적인 변화를 나타낸다. 이러한 차등적 변화가 정신증으로 점진적으로 이행하는 과정 기저의 신경생물학적 변화를 반영하는 것으로 생각된다.

핵심어: 정신증 초고위험군, 초발정신병, 확산텐서영상, 백질, 그래프 이론, 커넥톰

학번: 2010-30771